DESIGN AND DEVELOPMENT OF CRYOGENIC PUMPING EVALUATION FACILITY.

CARL M. ALBERO

DESIGN AND DEVELOPMENT OF A CRYOGENIC PUMPING EVALUATION FACILITY

* * * * *

Carl M. Albero

DESIGN AND DEVELOPMENT OF A CRYOGENIC PUMPING EVALUATION FACILITY

by

Carl M. Albero
Lieutenant, United States Navy

Submitted in partial fulfillment of
the requirements for the degree of

MASTER OF SCIENCE
IN
MECHANICAL ENGINEERING

United States Naval Postgraduate School
Monterey, California

1 9 6 5

DESIGN AND DEVELOPMENT OF A CRYOGENIC PUMPING EVALUATION FACILITY

by

Carl M. Albero

This work is accepted as fulfilling
the thesis requirements for the degree of
MASTER OF SCIENCE
IN
MECHANICAL ENGINEERING
from the
United States Naval Postgraduate School

ABSTRACT

A cryogenic pump is a cold surface employed to remove large volumes of gases from a vacuum system by condensing and freezing the gas molecules. Experimental results are presented for the cryopumping rate of carbon dioxide gas on a surface cooled by liquid nitrogen, and for nitrogen gas on a surface cooled by liquid helium. The nature of the problems encountered in the design and construction of a cryogenic pumping system are also discussed.

ACKNOWLEDGEMENTS

The work described herein was made possible by the continued support of the Office of Naval Research through the Foundation Research Program of the United States Naval Postgraduate School.

The author wishes to express his gratitude for the assistance and encouragement given him by Dr. Paul F. Pucci. He also wishes to thank Messrs. K. Mothersell, F. Abbe, K. Smith, and especially Mr. Joseph Beck for their technical assistance in the assembly and testing of the system.

TABLE OF CONTENTS

Section	Title	Page
1	Introduction	1
2	Cryopumping Theory	3
3	Description of Experimental Apparatus	14
4	Instrumentation	19
5	System Checkout Procedure	22
6	Experimental Technique	26
7	Uncertainty Analysis	28
8	Results	31
9	Analysis of Results	33
10	Conclusions	36
11	Bibliography	37
Appendix I	(a) System Dimensions	46
	(b) Liquid Nitrogen Feedthrough	47
Appendix II	Pumping System Operating Procedure	48
Appendix III	(a) Shielding Calculations	49
	(b) Cryopanel Calculations	52
	(c) Pumpdown Time Calculations	56
Appendix IV	(a) Vapor Pressure vs. Temperature for Common Gases	60
	(b) Outgassing Data	61
	(c) O - Ring Physical Properties	62

LIST OF ILLUSTRATIONS

Figure	Description	Page
1	Cryopumping Speed versus Temperature	9
2	Pressure versus Time	8
3	Pressure versus Time - CO_2 Flowrate (11.5 cc/min)	39
4	Pumping System Schematic	40
5	Cryopanel	41
6	Gas Addition System	42
7	Photograph - Front View of System	43
8	Photograph - Fill Plate	44
9	Photograph - Side View of System	45
10	Outgassing Rate versus Time	59

TABLES

1	Experimental Capture Coefficients of Nitrogen	32
2	Experimental Capture Coefficients of Carbon Dioxide	32
3	Reported Capture Coefficients of Carbon Dioxide	33

NOMENCLATURE

A	surface area	cm^2
C_p	specific heat at constant pressure	cal $gm^{-1} {}^\circ K^{-1}$
C	capture coefficient	------
E_b	emissive power	watts cm^{-2}
F	shape factor	------
G	mass flowrate unit area	gm cm^{-2} sec^{-1}
k	thermal conductivity	cal sec^{-1} cm^{-1} $^\circ K^{-1}$
L	latent heat of condensation from gas phase to solid phase for gaseous nitrogen	cal gm^{-1}
M	molecular weight	------
n	number molecules per unit volume	molecules cm^{-3}
N_o	Avagadro's Number	molecules mol^{-1}
$\dot{N}_s$	number of molecules striking a surface of unit area in a unit time	molecules cm^{-2} sec^{-1}
N	number of molecules initially present in the system	molecules
$\dot{N}_p$	fraction of molecules that adhere to the cryopanel per second	molecules cm^{-2} sec^{-1}
$(P_p)_c$	partial pressure of condensable gas	torr
p	chamber pressure	torr
Q	throughput rate	torr liters sec^{-1}
q	heat rate	watts cm^{-2}
R_m	universal gas constant	ergs $^\circ C^{-1} gm\text{-}mole^{-1}$
S_a	actual cryopumping speed	liters $sec^{-1} cm^{-2}$
S_{th}	theoretical cryopumping speed	liters sec^{-1} cm^{-2}
S_d	diffusion pumping speed	liters sec^{-1}
S	pumping speed	liters sec^{-1}

Nomenclature

T	temperature	°K
t	time	sec
V	volume	liters
$\dot{V}$	volumetric flowrate	$cm^3\ sec^{-1}$
V_a	average molecular velocity	$cm\ sec^{-1}$
ε	emissivity	------
σ	Stefan - Boltzmann constant	$watts\ cm^{-2}\ °K^{-4}$
ρ	density	$grams\ cm^{-3}$

Table of Subscripts

s	shield
r	conditions of residual in-leakage gas
o	conditions of induced in-leakage gas

1. Introduction

The requirement for large capacity space environmental chambers capable of operating in the 10^{-7} to 10^{-13} torr range has developed the need for a pump which will generate a high vacuum in a minimum time. Mechanical pumping facilities are not adequate due to the large size and cost of equipment necessary to pump down these chambers to the desired vacuum. In addition to the initial pump down, the problem of maintaining a high vacuum is compounded by the out-gassing characteristics of the materials inside the system and of the chamber walls, as well as the inevitable in-leakage from the atmosphere. The cryopumping technique for vacuum pumping has been investigated and proven to be more practical and economical than conventional vacuum pumping (1).[1]

Cryopumping removes gases from a system by condensing and freezing the gas molecules on a cold surface. This cold surface will pump any gas whose vapor pressure, at the temperature of the surface, is less than the ambient pressure within the system. For example, a cold surface at $20^{o}K$ will condense all gases present in a vacuum system except neon, hydrogen and helium.

The capture coefficient may be defined as the probability that a gas molecule with a given velocity, upon collision with a solid surface at a temperature below saturation at the ambient pressure, will adhere to the surface (5). Evaluation of the capture coefficient for various gases, on

[1] Numbers appearing in (parenthesis) indicate references listed in the Bibliography (pg 37)

surfaces maintained at cryogenic temperatures, has been the subject of recent research. The effect of surface geometry, surface temperature, surface condition and temperature of the gas being condensed have all been reported as affecting the capture coefficient (25, 26).

The cryopumping study presented in this paper was concerned with the evaluation of a 12" X 12" X ½" cryosurface. Experimental values for the capture coefficient were determined both for carbon dioxide gas and nitrogen gas on this surface.

2. Theory of Cryopumping

The study of cryopumping may be divided into the following categories;

(1) The vapor - solid interface

(2) Noncondensable gases

(3) The cryopanel surface and radiation shield

These categories are discussed below:

A. The Vapor - Solid Interface.

As the solid condensed gas forms on the cryosurface area, the thermal conductivity of this solid coating and its increasing thickness will affect further condensation of the gas.

Assume the refrigerant is maintained at constant temperature as the solid condensed gas accumulates on the cyrosurface. The temperature at the vapor - solid interface will then increase with time. Thus, the amount of gas condensed will decrease with time or in other words, the cryopumping speed will decrease with time.

In designing a cryosurface, the condensing surface area must be sufficiently large to provide adequate heat transfer through the solid condensed gas layer for the desired operating time. The design calculations for the cryosurface area used in this study are included in Appendix III b.

B. Noncondensable Gases.

The temperature of the cryosurface will determine which gases in the system will not condense. For example, at 77 ^{o}K the noncondensable gases are O_2, N_2, CO, Ne, H_2, and He. However, at 4 ^{o}K the only remaining noncondensable gas is He.

A practical and economical temperature used in most cryopumping installations is 20 ^{o}K. At this temperature H_2, He, and Ne are

noncondensable. It therefore becomes necessary to use a diffusion pump and mechanical pump in addition to a cryopump to remove the noncondensable gases.

C. Cryopanel Surface and Radiation Shield.

The principal heat load on the cryopanel surface is from radiation rather than from gas condensation at chamber pressures below 10^{-4} torr (5). It is therefore important that careful consideration be given to radiation shielding. The radiation shielding must also provide a low flow impedance to the cryopump surface. The requirement for low flow impedance and that for effective shielding are conflicting, except when one considers, in addition to these, the precooling of the gas before it reaches the pump surface. For most vacuum systems the gas to be pumped may be expected to be at room temperature or higher, the latter being the case for a low density hypersonic wind tunnel or for a high altitude rocket test cell. Mainly for the sake of conserving low temperature refrigeration (which is expensive to maintain), it is highly desirable to cool the incoming gas as close to the saturation point as possible before final contact with the cryopump surface. Another reason is that the gas temperature is actually the controlling factor for the capture coefficient at cryosurface temperature of 20 $^{\circ}$K or higher (29). Based on experimental evidence, the capture coefficient will increase as the gas temperature is decreased (29).

The functions of radiation shielding and precooling the gas can be combined in a system of cooled baffles (with liquid nitrogen, for instance) placed between the pump surface and the incoming gas.

An equation for computing the theoretical cryopumping speed based on the kinetic theory of gases will be developed.

From the kinetic theory of gases, the average molecular velocity can be derived (9).

$$V_A = \left[\frac{8 R_M T}{\pi M}\right]^{1/2} \quad \text{cm sec}^{-1} \tag{1}$$

where

V_A = average molecular velocity (cm sec^{-1})

R_M = universal gas constant (8.3146 X 10^7 ergs deg^{-1}K $g\text{-}mole^{-1}$)

M = molecular weight of gas

T = absolute temperature (°K)

If n is the number of molecules per unit volume, the number of molecules striking a surface in a unit time is (2)

$$\dot{N}_S = \frac{n V_A A}{4} = \frac{N}{V} \cdot \frac{V_A A}{4} \tag{2}$$

Then the fraction of the molecules which strike the cryopanel per second can be obtained from equations (1) and (2).

$$\frac{\dot{N}_S}{N} = \frac{A}{4V} \cdot V_A = \frac{A}{V}\left[\frac{R_M T}{2\pi M}\right]^{1/2} \tag{3}$$

As stated previously, the capture coefficient is the probability that a gas molecule with a given velocity (or equivalently energy), upon collision with a solid surface maintained at a temperature below saturation at the ambient pressure, will adhere to the surface (5).

The fraction of the molecules within the chamber that adhere to the cryopanel per second is

$$\frac{\dot{N}_P}{N} = \frac{C \dot{N}_S}{N} = \frac{CA}{V}\left[\frac{R_M T}{2\pi M}\right]^{1/2} \tag{4}$$

where

C = capture coefficient

$\dot{N}_p = C \dot{N}_s$

Since, by the kinetic theory, the pressure is proportional to the number of molecules per unit volume, the rate of pressure drop due to cryopumping is

$$\dot{P} = -\frac{PCA}{V}\left[\frac{R_M T}{2\pi M}\right]^{1/2} \tag{5}$$

where

V = chamber volume (cm^3)

P = chamber pressure (torr)

$\dot{P}$ = rate of pressure drop (torr sec^{-1})

The pressure rise due to the introduced in-leakage, $\dot{V}_o$, is

$$\dot{P}_o = \frac{R_M T}{V N_o}\frac{dN}{dt} = \frac{P_o \dot{V}_o}{V} \tag{6}$$

where

P_o = pressure of inlet gas (torr)

V = chamber volume (cm^3)

$\dot{V}_o$ = in-leakage per unit time (cm^3 sec^{-1})

The residual in-leakage is due to the in-leakage of air through seals, gaskets, etc., and outgassing of materials within the system. Outgassing is the release of gas by surfaces of the vacuum enclosure when a system is pumped down. The pressure rise due to residual in-leakage is

$$\dot{P}_r = \frac{P_r \dot{V}_r}{V} \tag{7}$$

Assuming the chamber to be isolated from any external pumping system and that equilibrium exists within the chamber, the rate of pressure decrease due to cryopumping is equal to the rate of pressure rise due to residual in-leakage plus introduced in-leakage. This can be expressed in equation form by utilizing equations (5), (6), and (7).

$$\frac{PCA}{V}\left[\frac{R_M T}{2\pi M}\right]^{1/2} = \frac{P_o \dot{V}_o}{V} + \frac{P_r \dot{V}_r}{V} \qquad (8)$$

Multiplying by the chamber volume, V, and assuming a value of the capture coefficient, C, equal to unity, equation (8) becomes

$$PA\left[\frac{R_M T}{2\pi M}\right]^{1/2} = P_o \dot{V}_o + P_r \dot{V}_r \qquad (9)$$

In vacuum technology, the product $P \cdot \dot{V}$ is defined as the throughput, Q. The throughput is simply the total in-leakage rate into the system at equilibrium. Utilizing this definition equation (9) becomes

$$PA\left[\frac{R_M T}{2\pi M}\right]^{1/2} = Q \qquad \text{torr cm}^3 \text{ sec}^{-1} \qquad (10)$$

The cryopanel pumping speed is defined as the volume flow rate, at chamber pressure, condensed per unit area of the cryosurface (5).

$$S = Q/PA \qquad (11)$$

From equation (10) we may then express the cryopumping speed as

$$S_{th} = \left[\frac{R_M T}{2\pi M}\right]^{1/2} \qquad \text{cm}^3 \text{ sec}^{-1} \text{cm}^{-2} \qquad (12)$$

where S_{th} denotes the theoretical cryopumping speed, since it was assumed previously that the capture coefficient was unity. Equation (12) can be expressed as follows:

$$S_{th} = \left[\frac{R_M T}{2\pi M}\right]^{1/2} \cdot 10^{-3} \quad \text{Liter sec}^{-1}\text{CM}^{-2} \tag{12a}$$

Using equation (12a), the theoretical cryopumping speed may be computed for common gases as a function of introduced gas temperature. Fig. (1) on the following page is a plot of theoretical cryopumping speed versus temperature for common gases.

The experimental method employed may be made more clear by a discussion of some of the working mechanisms which occur during cryopumping. After describing these mechanisms, an equation for calculating the actual cryopumping speed and capture coefficient of a cryosurface will be developed.

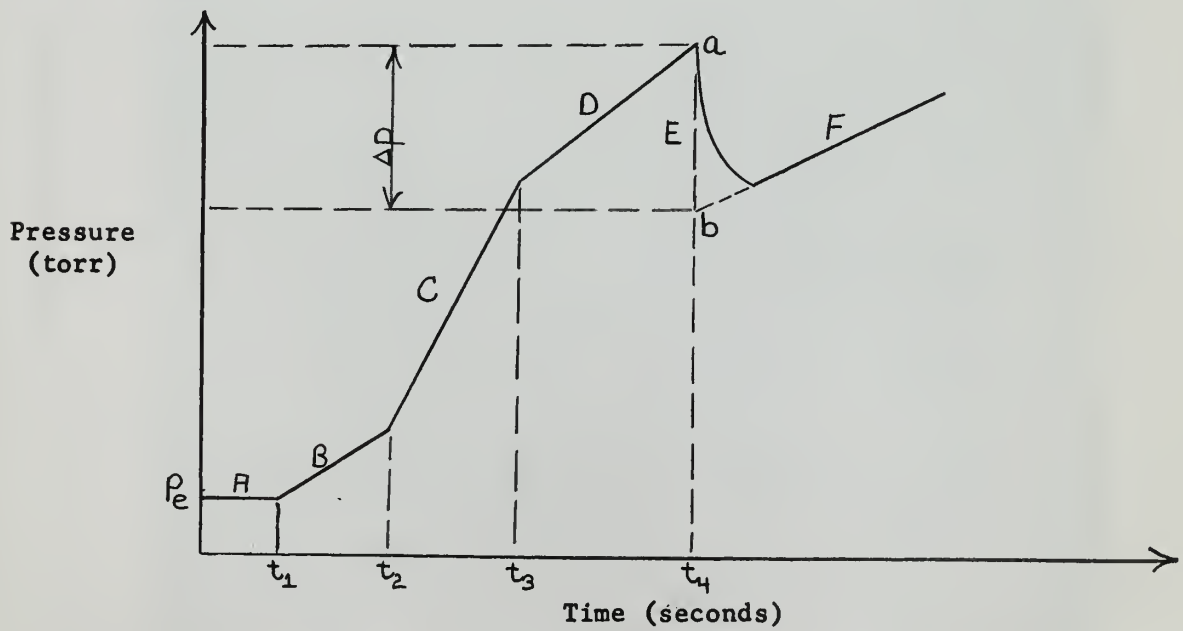

Figure 2 Pressure versus Time

Figure 1

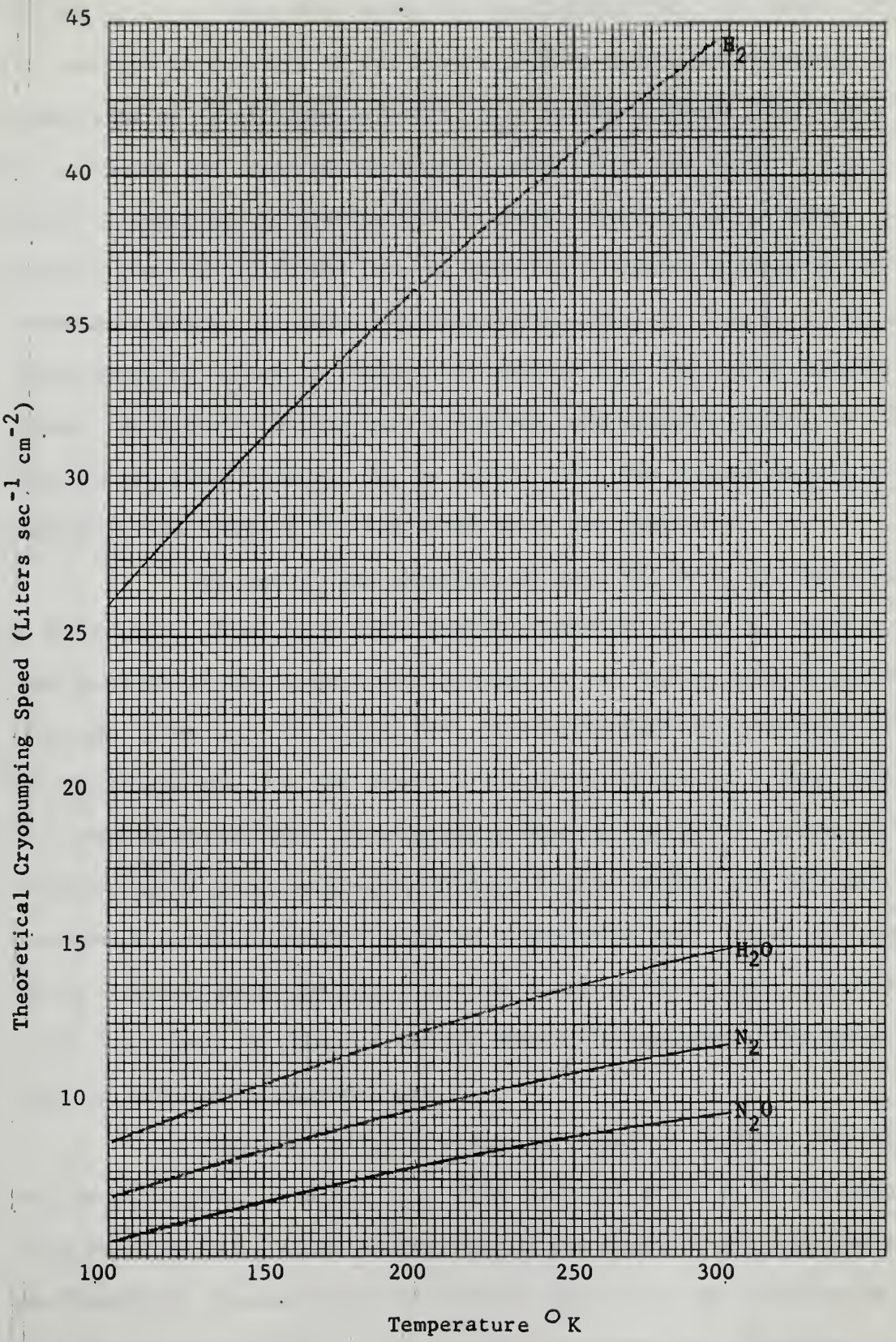

Cryopumping Speed vs. Temperature

Figure (2) is a typical chamber pressure versus time curve plotted by an X-Y recorder during an experimental run. In region "A", the pressure is constant as the vacuum pumping system and cryopumping have established an equilibrium pressure, p_e , in the chamber. The cryosurface is condensing and freezing condensable gases while the vacuum pumping system is removing the noncondensable gases. However, it is also possible that the diffusion pump is removing a certain portion of the condensable gases. To eliminate this possibility, at time t_1 a high vacuum valve is closed to isolate the chamber from the vacuum pumping system. As equilibrium has been disturbed, the pressure starts to rise from its equilibrium valve, P_e, in region "B". The cryosurface is now condensing and freezing all the condensable gas molecules.

At time t_2 the experimental gas, CO_2 or N_2 in this study, is introduced. There is a rapid pressure rise in region "C" until the pumping speed of the cryosurface is equal to the inflow rate of condensable gas (time t_3). In region "D", the cryosurface is condensing all of the introduced gas, but the pressure continues to rise at a less rapid rate than in region "C". This pressure rise in region "D" is due to the non-condensable gases originally present in the chamber and the non-condensable gases introduced with the condensable gas. Since all commercially produced gases contain a certain amount of impurities, about 1 part in 10^7 (5), there is always a certain amount of noncondensable gases introduced with the condensable gas.

When the inflow of condensable gas is secured, the pressure will drop abruptly in region "E". This pressure drop, $\triangle$ P, has been found experimentally to be independent of the duration of condensable gas flow (26). In measuring the pressure drop, $\triangle$ P, the time lag in securing the gas admission valve must be accounted for. Therefore, the

pressure rise in region "F" is extrapolated back to time t_4. The pressure drop is then measured from a to b as shown in Fig. 2.

When the condensable gas flow is secured, according to Dalton's law of partial pressures, the pressure in the chamber will decrease by an amount equal to the partial pressure of the condensable gas. Dalton's law can be applied to the present experimental method provided

$$(P_p)_c \gg (P_p)_{NC} \tag{13}$$

If the condition expressed by equation (13) is not satisfied

$$(P_p)_c > \Delta P \tag{13a}$$

The reason is the condensable gas flowing into the chamber will undergo a momentum exchange with the non-condensable gases present. This will tend to increase the density of the non-condensable gases in the direction of flow. Upon securing the condensable gas flow, the non-condensable gases will expand to fill the chamber uniformly, and the observed pressure drop, Δ P, will be less than the partial pressure of the condensable gas before cut-off.

A working equation for calculating the actual cryopumping speed will now be developed based on measuring the partial pressure of the introduced gas under equilibrium conditions (26). Equilibrium exists at time t_3 (see Fig. 2). At this time, as stated previously, the cryosurface is condensing all the condensable gases flowing into the chamber. The condensable gas throughput into the chamber at time t_3 is

$$Q_c = (P_o \dot{V}_o)_c + (P_r \dot{V}_r)_c \qquad \text{torr liter sec}^{-1} \qquad (14)$$

All the terms in equation (14) have been defined previously. The subscript c, denotes condensable gas.

If the condensable gases being emitted from the inner chamber walls are assumed negligible in comparison with the introduced condensable gas, equation (14) may be simplified as follows:

$$Q_c = P_o \dot{V}_o \qquad \text{torr liter sec}^{-1} \qquad (14a)$$

Substituting Q_c from equation (14a) for the throughput in equation (11), an equation for calculating the actual cryopumping speed is obtained.

$$S_A = \frac{P_o \dot{V}_o}{PA} \qquad \text{Liter sec}^{-1}\text{cm}^{-2} \qquad (15)$$

If no non-condensable gases were present in the chamber, the chamber pressure would remain at a constant value when the cryosurface was condensing and freezing all the introduced condensable gas. This value would be used for the pressure, P, in equation (15). However, the chamber is isolated from the vacuum pumping system during the experimental run, and therefore the non-condensable gases cannot be removed from the chamber. This precludes a direct measurement of the pressure, P.

The partial pressure of the condensable gas is equivalent to the measured pressure drop, $\triangle$ P, provided equation (13) is satisfied. Further, the partial pressure of the condensable gas may be used for the chamber pressure, P, in equation (15) when the saturation vapor pressure of the solid condensate, P_s, is much less than the partial pressure of

the in-flowing gas.

$$(P_p)_c \gg P_s \tag{16}$$

If ΔP approaches P_s the interference of non-condensable molecules, as well as re-emitting condensable molecules from the solid condensate, will become significant. Therefore, the condition expressed by equation (16) must be true for the experimental method employed to produce accurate results.

To summarize:

If

1) $(P_{pc} \gg (P_p)_{NC}$ (13)

2) $(P_p)_c \gg P_s$ (16)

then

1) $\Delta P = (P_p)_c$

2) P in equation 15 = $(P_p)_c$

and equation (15) becomes

$$S_A = \frac{P_o \dot{V}_o}{(P_{pc} A} \tag{17}$$

Equation (17) is the working equation utilized to calculate the actual cryopumping speed. The capture coefficient can now be obtained from (12a) and equation (17) as follows:

$$C = \frac{\frac{P_o \dot{V}_o}{(P_p)_c A} \cdot 10^3}{\left[\frac{R_M T}{2\pi M}\right]^{1/2}} \tag{18}$$

3. Description of Experimental Apparatus

a) Vacuum System

The vacuum chamber used in this study was a modified 40 inch diameter vacuum furnace manufactured by National Research Corporation. The actual modification of this chamber was performed by LT G. M. LaChance and is described in detail in (16). For the vacuum pumping system schematic see Fig. 4.

A 6 inch, 4 stage, fractionating, diffusion pump capable of pumping 1500 liters/sec and with an ultimate blank-off pressure of 10^{-7} torr was used to pump down the chamber. This pump was backed by a 100 CFM, single-stage mechanical pump. The diffusion pump was charged with a silicone diffusion pump fluid, Dow Corning 704. Under operating conditions the diffusion pump requires a power input of 1500 watts to the heating element and requires 2.91 lbs/min of cooling water. A thermistor switch was mounted on the pump body and will automatically secure the power to the heaters in event of a cooling water failure.

In order to reduce back streaming, a 6 inch liquid nitrogen optically dense baffle manufactured by National Research Corporation was installed above the diffusion pump. This baffle requires a charge of 1000 cc of liquid nitrogen every 4½ hours. In addition to reducing back streaming, this baffle will condense certain gases being pumped from the chamber and therefore reduce the pumping load on the diffusion pump. A cold cap was also installed on the top jet of the diffusion pump to aid in reducing back streaming. However, examination of the bottom surface of the nitrogen baffle showed considerable diffusion pump oil. It is the opinion of the author that this cold cap could be removed from the system without causing any adverse effects.

Directly above the liquid nitrogen baffle and mounted below the chamber was a 6 inch high vacuum, air actuated, solenoid operated valve manufactured by Vacuum Research Corporation. This valve will open or close in less than two seconds and is certified for a leak rate of 1×10^{-9} std/cc/sec. It is also equipped with Viton O-rings in order to minimize outgassing. In event of power failure, this valve will close and isolate the chamber from the pumping system. The combined conductance of this valve, the liquid nitrogen baffle, and diffusion pump is 600 liters/sec. It may be checked by performing a rate-of-rise measurement on the chamber (22).

All flanges between the chamber and the diffusion pump are fitted with Viton O-rings to reduce outgassing. It is recommended that vacuum grease not be used on Viton Orings as they have a much lower vapor pressure than the grease itself.

The foreline piping is 1½ inch seamless 304 stainless steel tubing. The foreline valve is an air actuated, solenoid operated valve manufactured by National Research Corporation. It will close in event of power failure or loss of air supply. This feature protects the foreline piping from mechanical pump oil contamination and also prevents the exposure of the hot diffusion pump oil to the atmosphere. All flanges in the foreline piping were manufactured with a 32 r.m.s. finish and O-ring grooves .005 inches less in depth than a standard groove. Experience has proven that this combination will work best.

The roughing piping is connected directly to the chamber. The size of this line is 3 inch stainless steel 304 tubing and the foreline valve is a manually operated 3 inch bellows sealed valve. The foreline piping cuts into the roughing piping aft of this manual 3 inch valve.

b) Cryopanel

In previous cryopump studies the refrigerant was recirculated in a closed loop through the cryopanel then to a cryostat for re-cooling (19). This was not feasible in this study as a cryostat was not available. Therefore a "batch process" cryopump was constructed. This method enables the use of a less sophisticated transfer system for the liquid helium. However, the liquid helium once vaporized in the panel is not recoverable. The vaporized helium is replaced with another charge when the cryopanel begins to warm. The cryopanel configuration is shown in figure (5).

The material chosen for construction of the cryopanel was type 304 stainless steel. This type steel affords the advantages of low outgassing, high tensile strength and good ductility at low temperature.

The cryopanel designed and installed for this study was a rectangular box arrangement, 12" X 12" X ½". Four stiffners are installed between the two 12" X 12" surfaces. These members were constructed by heli-arc welding two channel sections together and spot welding the resulting box arrangement to each surface. Including the fill and vent piping, the cryopanel weighs three (3) pounds.

Under operating conditions the pressure inside the panel is approximately 15 psia (atmospheric pressure plus pressure head due to cold fluid) while the outside surface is exposed to the vacuum chamber pressure (1×10^{-6} to 1×10^{-8} mm Hg). Therefore, prior to installation the panel was tested hydrostatically by blanking off the vent line to the panel and pressurizing the panel to 35 psia. At the time of this test, the outside surfaces of the cryopanel were exposed to atmospheric pressure so that a 20 psi pressure differential existed across each wall of the panel. The

cryopanel was also leak checked with a Veeco mass spectrometer type leak detector. This test was performed by pumping on the inside volume of the cryopanel with the leak detector pumping system. The outside surface of the cryopanel was covered with a plastic bag and the bag was then filled with gaseous helium. When no discernible in-leakage of helium gas was observed, the cryopanel was accepted for installation.

c) Radiation Shielding

The chamber walls are at essentially room temperature while the cryopanel temperature is approximately 20 ^{o}K. Since the operating pressure of the chamber is in the 10^{-8} torr range, it can be assumed that the principle heat load on the panel is due to radiation. Therefore, a radiation heat shield maintained at a lower temperature, installed between the cryopanel and chamber walls would greatly reduce the liquid helium consumption in the cryopanel. A liquid nitrogen shield cooled to approximately 77 ^{o} K was installed between the chamber walls and cryopanel. In this manner the radiation heat load on the cryopanel was reduced to approximately 0.4% of the value without shielding (Appendix IIIa). A detailed description of the liquid nitrogen shielding utilized in this thesis is presented in (16).

The liquid nitrogen consumption in the primary heat shield can be reduced by installing a dry aluminum shield. Such a shield was installed between the chamber walls and the cylindrical liquid nitrogen shield. The radiation heat load on the primary shield was reduced to about 25% of its unshielded value with this method (App. IIIa).

The following modifications were performed to the liquid nitrogen fill system described by LT G. M. LaChance in (16):

a) The vent lines from the cylindrical heat shield and the back shield were increased in size from 3/4" to 1".

b) A separate vent line was installed for both the cylindrical and back shield.

c) The fill plate arrangement at the top of the chamber was redesigned as were the liquid nitrogen feed-throughs. (See App. Ib)

d) The cylindrical heat shield and back heat shield piping were modified to permit the filling of each shield separately.

e) A manifold with quick closing ball valves was installed in the liquid nitrogen transfer line.

f) Nylon hoses were inserted in the fill lines to enable releasing the liquid nitrogen as close to the bottom of the shields as possible.

4. Instrumentation

a) Pressure

Two types of gages were used to monitor the pressures in the system, a Bayard - Alpert type ionization gage to measure the pressures below 10^{-3} torr and thermocouple gages for pressures above 10^{-3} torr. A McLeod gage was utilized to calibrate the Veeco thermocouple gage controller.

An X-Y recorder, model 2A, manufactured by the F. L. Mosely Co., was connected to the output therminals at the rear of the chassis on the Veeco controller. The impedance of the recorder matches the one specified for the controller amplifier, 2000 ohms or greater, and is ideal for this application. The recorder can also generate its own time scale along the x-axis. Since the output of the controller amplifier is 2 volts for full scale deflection on the ionization gauge meter, the recorder was calibrated so that a .02 volt output from the controller amplifier was equivalent to 1×10^{-6} torr. During all CO_2 test runs the Veeco scale selector switch was placed on the 10^{-5} torr scale. This made it possible to record an experimental run without switching scales on the Veeco.

The controller - recorder combination is accurate within 2% of the controller full scale deflection. When operating on the 10^{-5} scale, the maximum possible error is therefore 0.2×10^{-5} torr. Full scale deflection on the 10^{-5} scale is 10×10^{-5} torr.

b) Temperature

The temperature sensing devices utilized were thermocouples and disk thermistors. Type L0904 - 125K - H - T2 disk thermistors manufactured by Keystone Carbon Co., were used to measure surface temperatures at

certain locations on the liquid nitrogen filled heat shields. These thermistors were individually calibrated by the manufacturer at 90 ^{o}K, 77.1 ^{o}K, and 20.2 ^{o}K. One, type L0904 - 3meg - He - T2 disk thermister, was used on the cryosurface. This thermister was calibrated by the manufacturer, Keystone Carbon Co., at 90 ^{o}K, 77.1 ^{o}K, 20.2 ^{o}K, and 4.1 ^{o}K. It was used to measure temperatures in the liquid helium range. A typical calibration curve for these thermistors is included in reference (16).

Teflon insulated 24 gauge copper - constantan thermocouples were employed. These thermocouples were installed on the front heat shield, the top of the cylindrical shield, the liquid helium fill line, the liquid helium cryopanel bottom center, and the liquid helium cryopanel vapor outlet. A liquid nitrogen reference junction was used to improve the thermocouple sensitivity at temperatures below 77 ^{o}K. The data employed to convert millivolts to a corresponding temperature utilizing a liquid nitrogen reference junction for copper - constantan thermocouple wire was obtained from reference (28).

The thermocouples were mounted on the surface by spot welding a piece of stainless steel shim stock over the measuring junction. Apiezon-N grease was used to bond the junction to the surface with a reasonable degree of success. Apiezon-N grease has a low vapor pressure and will harden at low temperature. This hardening tends to keep the thermocouple in contact with the surface and reduce any error in the temperature reading due to poor contact. It was found that thermocouples making poor contact with the surface could register temperatures which were as much as 20 ^{o}K in error.

As stated above, the thermistors, two of which were used on the

back shield and one on the cryopanel, are discussed in (16). The only modification made to the thermistors was in the method of mounting them to the surface. Instead of utilizing Sauereisen Type 29 "Low Expansion Cement", which outgasses heavily, the thermistors were wrapped in teflon tape and held to the surface with stainless steel shim stock spot welded to the surface. In mounting the thermistors, it was found that grounding would occur if the disk was not insulated from the surface with teflon tape. Apiezon-N grease was used to insure contact between surface and thermistor.

The liquid nitrogen thermistors were immersed in a bath of liquid nitrogen for calibration and the bath agitated to prevent stratification. These thermistors were all approximately -10 ^{o}K in error. This is in agreement with the reported observation in reference (16).

c) Flow Measuring Devices

The schematic of the gas admission system is displayed in Figure 6. Nitrogen and carbon dioxide gas flow into the chamber was controlled with a micro-flow valve manufactured by the Matheson Company, Inc. This valve is vacuum tight to 10^{-6} torr and for a 2 psi pressure differential is capable of metering flows in the range of 0.25 cc/min to 6,000 cc/min of air. Since this valve has a very small orifice, it was equipped with a filter to prevent it from clogging.

The flowmeter employed has a high precision glass ball float 3/64" in diameter and allows for a reproducibility of better than one scale division on the meter. The flowmeter has a range of 1 cc/min to 100 cc/min.

5. System Checkout Procedure

a) Obtaining a Vacuum Tight System

The vacuum pumping system was valved and instrumented to provide maximum operating flexibility and to permit leak checking in small isolated sections. In the following discussion reference to the pumping schematic (Figure 1) will aid the reader in understanding the procedures described.

In vacuum technology, the piping from the diffusion pump discharge to the mechanical pump inlet is referred to as the foreline piping. In this discussion the foreline piping will include all components from the vacuum test chamber to the mechanical pump inlet. This section was initially pumped down with the mechanical pump and checked with a Veeco mass spectrometer type leak detector using helium as the probing gas. After all detectable leaks had been corrected, a pressure in the foreline piping of 5 microns was realized. The diffusion pump was placed in operation, and the foreline piping was again checked for a discernible in-leakage. This operation was performed to insure the components and flange connections between the chamber and inlet to the diffusion pump were leak tight at a high vacuum. A leak was detected at the flange connection between the cold cap and diffusion pump proper. Upon correcting this difficulty, the leak detector showed no discernible in-leakage of helium on the most sensitive scale.

The chamber was tested next with valve V-3 open and valves V-2 and V-1 closed. The leak detector was connected via valve V-5 to the vacuum system. It was possible to rough down the chamber to 10 microns in this manner with no detectible leaks. It was noted that the chamber required approximately 1½ times as long to rough down if it had been opened for any appreciable time. This is due to a layer of water molecules

forming on the chamber walls when exposed to the air. Therefore, it became standard procedure to place lamps in the chamber if it was to be open for any duration of time. Also, the system was raised to atmospheric pressure with nitrogen gas upon securing under the following conditions:

1) The chamber was not going to be opened for maintenance.

2) The chamber was to be idle for a short period of time and it was desired to come back down to pressure rapidly.

The last step in checking out the system was to test it as a whole unit. It was placed in operation by following the procedure outlined in App. II. The leak detector was connected to valve V-4 and valve V-2 was closed. Note that with valve V-2 closed, the diffusion pump is discharging solely to the leak detector. This enables almost instant response to a leak. Once the leaks were remedied, a vacuum of 9×10^{-7} torr was realized without the addition of any cold liquids. By filling the cold cap, two liters of liquid nitrogen required, a vacuum of 8×10^{-7} torr was obtained. At this stage, no leaks were detectible with the leak detector on the most sensitive scale. The vacuum system was accepted and it was now possible to proceed with testing the heat shielding.

b) Testing the Liquid Nitrogen System

The heat shields and cryopanel were leak checked before installation within the chamber. Upon filling these shields with liquid nitrogen, numerous problems developed.

The front door shield fill operation was uneventful. However, initially it was impossible to fill the back and cylindrical shields without a loss of vacuum within the chamber. This was attributed to the O-rings freezing on the fill plate and a sharp 90 degree bend at the fill line entrance. Difficulty was also encountered with silver solder joints connecting flexible stainless tubing to the rigid tubing. These joints were

a constant source of trouble due to leaks developing at liquid nitrogen temperatures. Also it was not possible to fill at a reasonable rate due to liquid bubbling out of the fill line on to the plate whenever the pressurizing gas was increased above ¼ psig.

The following steps were taken to eliminate the above mentioned problems:

1) The viton O-rings on the fill plate were replaced with silicone O-rings. This lowered the freezing temperature of the O-rings from + 4 ^{o}F to -90 ^{o}F.

2) The liquid nitrogen fill piping was modified to allow filling the back shield and cylindrical shield separately.

3) A sweeping bend was used instead of a sharp 90 degree bend in the fill piping.

4) A nylon hose was inserted in the fill pipe for the cylindrical shield. This enabled the liquid nitrogen to be released at the bottom of the shield and provided a long conduction path thereby reducing the vapor present in the fill line. It also served to keep the fill plate warmer. Holes were drilled in the sides of the hose ½" from the bottom to allow for the eventuality of the hose outlet resting on the bottom of the shield.

5) The vent lines were modified so that cold vapor was discharged away from the fill plate.

6) Electrical resistance tape was placed on the plate around the O-rings. A current of .5 amps from a 115 volt supply was passed through this tape. As a result 60 watts of power were available to heat the plate while the fill operation was proceeding.

7) Self pressurized dewars were used in the actual test

runs. A device was designed to exert a slight pressure on the fill line and to prevent bubbling from this line. This device is shown in Appendix I b.

These modifications were successful and the fill time required was 45 minutes. The reader is referred to (21), Chapter VIII, for an outstanding discussion of two phase flow in transferring cryogenic liquids. Scott (21) also recommends vapor taps in the fill line to relieve the pressure and enable the liquid to move more rapidly thereby cooling the line.

c) Testing the Liquid Helium Panel.

The liquid helium cryopanel was filled through a 33 inch vacuum insulated transfer line. No difficulty was encountered with this operation and as the procedure is a standard one in the field, it will not be discussed further here.

6. Experimental Technique.

(1) Pump down the vacuum chamber to the lowest possible pressure with the mechanical and diffusion pumps.

(2) Fill the radiation shields with liquid nitrogen. During the fill operation, monitor the level of the liquid nitrogen with the installed thermistors and thermocouples. The time required to fill the heat shields with liquid nitrogen is approximately 45 minutes. About 50 liters of liquid nitrogen are required.

(3) Upon completion of the fill operation, record all heat shield temperatures, cryopanel temperature, and chamber pressure.

(4) When CO_2 gas is to be condensed on the cryopanel, step (2) and (3) above are omitted.

(5) Fill the cryopanel with liquid helium or liquid nitrogen depending on whether CO_2 gas or N_2 gas is to be condensed. When using liquid helium, the cryopanel temperature must be monitored continuously. If the cryopanel temperature starts to rise above $20^{\circ}K$, introduce more liquid helium to the cryopanel.

(6) Record temperatures of the cryopanel and heat shields.

(7) Record the chamber pressure (P) obtained by cryopumping.

(8) Isolate the diffusion pump from the chamber by closing valve V-1. (See Fig. 4).

(9) Record Pressure versus Time with the X-Y plotter.

(10) Introduce a known in-leakage rate with the gas metering system. (See Fig. 6)

(11) Record the pressure and temperature of the introduced gas.

(12) The in-leakage may be secured after time t_2. (Fig. 2 is repeated below for convenience).

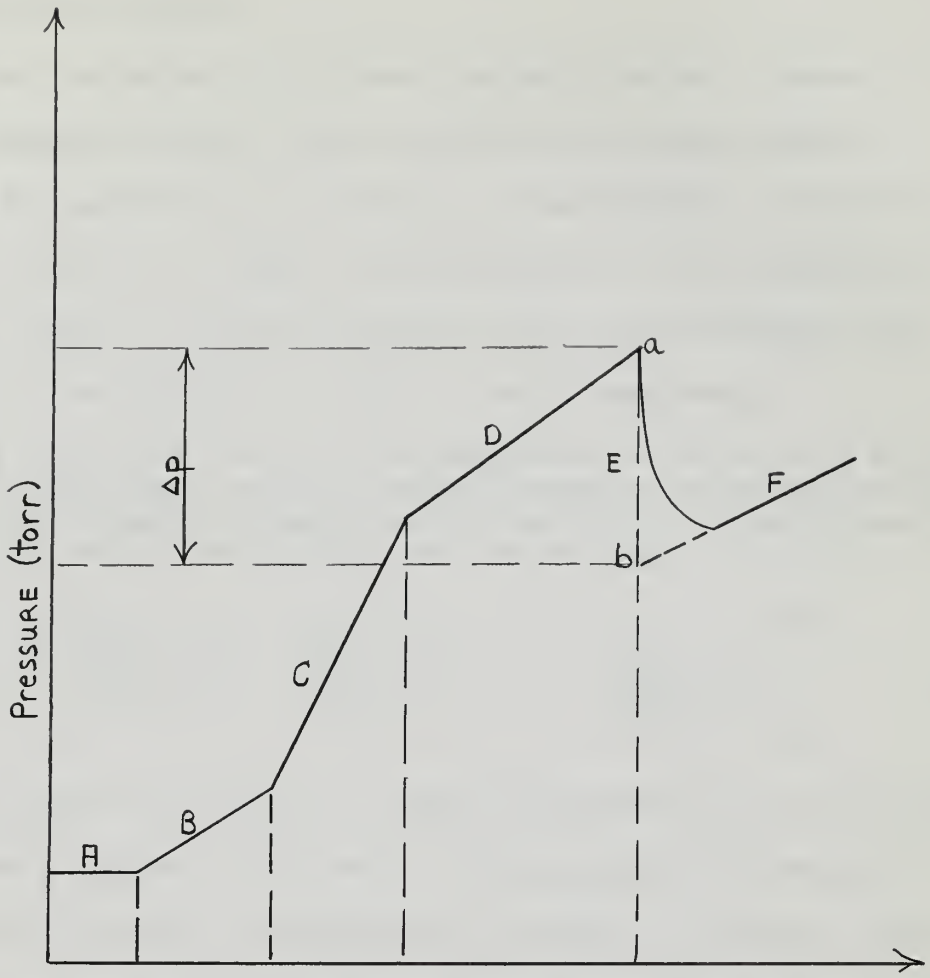

Fig. 2 Pressure versus Time

(13) After the pressure drop Δp has been observed, open valve V-1 and restore the chamber pressure (P).

(14) Compute the cryopumping speed as follows:

$$S_A = \frac{P_o \dot{V}_o}{(p)_c A}$$

(15) Calculate the capture coefficient as follows:

$$C = \frac{S_A \cdot 10^3}{\left[\frac{R_M T}{2\pi M}\right]^{1/2}}$$

7. Uncertainty Analysis.

The data collected in this study was mostly single - sample. A single - sample experiment is one in which uncertainties cannot be evaluated by repetition due to the cost or time involved. Therefore the author will provide the reader with some measure of the reliability of the results based on a method developed by Kline and McClintock (31) for analyzing uncertainties in single - sample experiments.

"If R is a linear function of N independent variables, each of which is normally distributed, then the relation between the interval for the variable w_i , and the interval for the result w_R , which gives the same odds for each of the variables and for the result is" (31)

$$w_R = \left[\left(\frac{\partial R}{\partial V_1} w_1 \right)^2 + \left(\frac{\partial R}{\partial V_2} w_2 \right)^2 + \cdots\cdots \left(\frac{\partial R}{\partial V_N} w_N \right)^2 \right]^{1/2} \qquad (1)$$

The above theorem will be used to report the uncertainty for each experimental result reported in this work. The uncertainty interval will be based on 20 to 1 odds. In other words, the author is willing to wager 20 to 1 that the true value for the experimental result lies within the uncertainty interval stated.

A sample calculation for one run will now be performed utilizing the following data:

$\dot{V}_0 = 11.50$ cc/min

$A = 2165$ cm^2

$(P_{pc}) = 1.2 \times 10^{-5}$ mm Hg

$P_0 = 760$ mm Hg

The uncertainties, w_i , for the above mentioned data are:

in $\dot{V}_0 = 1.0$ cc/min

in $A = 152$ cm^2

in $(P_{pc}) = 0.05 \times 10^{-5}$ mm Hg

in P_0 = negligible

The equation employed for calculating the experimental pumping speed is

$$S_A = \frac{P_o \dot{V}_o}{(P_p)_c A} \tag{2}$$

The experimental pumping speed S_A corresponds to R and is a linear function of the independent variables V_o, $(P_p)_c$ and A. Substituting equation (2) into equation (1) and performing the indicated partial differentation:

$$W_{S_A} = \left[\left(\frac{P_o W_{\dot{V}_o}}{(P_p)_c A} \right)^2 + \left(\frac{P_o \dot{V}_o W_p}{A (P_p)_c} \right)^2 + \left(\frac{P_o \dot{V}_o W_A}{A^2 (P_p)_c} \right)^2 \right]^{1/2} \tag{3}$$

Equation (3) can be normalized upon dividing by equation (2)

$$\frac{W_{S_A}}{S_A} = \left[\left(\frac{W_{\dot{V}_o}}{\dot{V}_o} \right)^2 + \left(\frac{W_{(P_p)_c}}{(P_p)_c} \right)^2 + \left(\frac{W_A}{A} \right)^2 \right]^{1/2} \tag{3a}$$

Substituting the values for the variables and uncertainties into equation (3a)

$$\frac{W_{S_A}}{S_A} = \left[\left(\frac{1.0}{11.5} \right)^2 + \left(\frac{.05}{1.2} \right)^2 + \left(\frac{152}{2200} \right)^2 \right]^{1/2}$$

$$\frac{W_{S_A}}{S_A} = 0.119$$

Therefore, we see that the experimental cryopumping speed is 11.9% uncertain. The uncertainty interval for this run is

$$\frac{W_{S_A}}{S_A} = \frac{W_{S_A}}{5.6 \text{ (Liter/sec cm}^2\text{)}} = 0.119$$

$$W_{S_A} = 0.67 \text{ Liter/sec cm}^2$$

where the value for S_A was computed from equation (2). Therefore, the experimental cryopumping speed is reported in the following form:

$$S_A = 5.60 \pm 0.67 \ \text{Liter/sec cm}^2$$

The capture coefficient uncertainty interval is directly proportional to the uncertainty in the experimental cryopumping speed. By definition the capture coefficient is

$$C = \frac{S_A}{S_{th}} = \frac{5.60 \pm 0.67}{9.53}$$

or

$$C = 0.59 \pm 0.07$$

8. Results.

The cryopumping speed for various flowrates of CO_2 gas at 300 ^{o}K was determined for a cryosurface maintained at 77 ^{o}K by liquid nitrogen. For each cryopumping speed measured experimentally, a capture coefficient was calculated. Equation (13) of Chapter I was employed to compute the experimental pumping speed and equation (14) of the same chapter was utilized to calculate the capture coefficient. A value of 9.53 Liter/cm^2 sec was obtained from Fig. 1 for the theoretical cryopumping speed of CO_2 at 300 ^{o}K. Equations (17) and (18) are repeated below:

$$S_A = \frac{P_o \dot{V}_o}{(P_p)_c A} \tag{17}$$

$$C = \frac{S_A}{S_{th}} \tag{18}$$

Figure 3 illustrates a typical pressure versus time record for a CO_2 flowrate of 11.5 cc/min. Table II(page 32), shows the experimental data and the calculated capture coefficients for CO_2. All values are based on a cryosurface area of 2165 cm^2.

The cryopumping speed for nitrogen gas at 300 ^{o}K was also determined for a cryosurface cooled by liquid helium. The same equations employed for carbon dioxide were also used for nitrogen. The capture coefficient was computed for nitrogen utilizing a value of 11.9 Liters/sec cm^2 (See Fig. 1) for the theoretical cryopumping speed. Table I below shows the experimental data and the calculated capture coefficients for nitrogen. The cryosurface temperature was 10 ^{o}K ($\pm$ 5 ^{o}K).

TABLE I

$\dot{V}_o$	Area	$(P_P)_c$	S_A	Capture Coefficient	Uncertainty of Capture Coeff.
cc/min	cm^2	(torr)	Liter/am^2sec		
1.0	2165	7.19×10^{-7}	8.14	0.68	0.52
9.0	2165	5×10^{-6}	10.5	0.88	0.14

TABLE II

Run No.	$\dot{V}_o$ (cc/min)	$(P_P)_c$ Torr	S_A Liters/cm^2sec	Capture Coefficient	Uncertainty of Capture Coeff.
1	4.52	4×10^{-6}	6.6	0.69	0.12
2	5.74	4×10^{-6}	8.4	0.88	0.15
3	5.74	4.2×10^{-6}	8.0	0.84	0.13
4	6.64	5.5×10^{-6}	7.1	8.74	0.10
5	7.38	5.9×10^{-6}	7.3	0.77	0.10
6	8.62	7×10^{-6}	7.2	0.76	0.10
7	11.50	1.1×10^{-5}	6.1	0.64	0.08
8	11.50	1.2×10^{-5}	5.6	0.59	0.07
9	11.50	1.2×10^{-5}	5.6	0.59	0.07
10	11.50	1.2×10^{-5}	5.6	0.59	0.07
11	15.60	1.7×10^{-5}	5.5	0.58	0.07
12	2.87	2.5×10^{-6}	6.7	0.70	0.17
13	2.87	2.5×10^{-6}	6.7	0.70	0.17

With liquid helium cryopumping, a minimum pressure of 5×10^{-8} mm Hg was realized for a cryosurface temperature of 10^{o}K. This value is for continuous noncondensable gas removal and with no introduced gas in-leakage.

9. Analysis of Results.

Values reported in the literature for the capture coefficient of carbon dioxide gas at 300 ^{o}K, based on experimentally measured cryopumping speeds, on a liquid nitrogen cooled surface are displayed in Table III below. The cryosurface geometry utilized in all cases was a sphere.

TABLE III

CO_2 Flowrate, $\dot{V}_0$ cc/sec	P (Torr)	Capture Coefficient	Reference
0.525	1×10^{-4}	0.42	(26)
2.17	3×10^{-4}	0.63	(26)
0.418	0.7×10^{-4}	0.58	(26)
2.22	3.1×10^{-4}	0.70	(26)
0.105	1.1×10^{-4}	0.63	(26)
0.105	1.2×10^{-4}	0.57	(26)
- - - -	- - - - - -	0.63	(29)
- - - -	- - - - - -	0.63	(30)

Examination of the capture coefficients for CO_2 computed from the experimental cryopumping speeds in this report compare favorably with those reported in the literature, for equilibrium chamber pressures in the 10^{-5} Torr range. As stated previously, in Chapter I, the partial pressure of the introduced condensable gas, $(P_p)_c$, is equivalent to the equilibrium chamber pressure provided the following conditions are true:

(1) The saturation vapor pressure of the solid condensate is much less than the partial pressure of the introduced gas.

(2) The partial pressure of the introduced gas is much greater than the partial pressure of the noncondensable gases present in the test chamber.

For chamber equilibrium pressures in the 10^{-6} Torr range, the capture coefficients are higher than most of the reported values in the literature. This discrepancy may possibly be attributed to:

1) A larger uncertainty in the pressure measurement, ΔP, in the 10^{-6} Torr range than in the 10^{-5} Torr region.

2) The effect of noncondensable gases.

Although it is very difficult to determine accurately the partial pressure of the non-condensable gases in the chamber without a mass spectrometer, the partial pressure can be estimated by performing a rate of pressure rise measurement on the chamber (22). A value of 1×10^{-6} Torr for the partial pressure of the noncondensable gases was obtained in this manner. Since this is the same order of magnitude as the equilibrium chamber pressure, it can be assumed that the non-condensable gases did increase the measured cryopumping speed and therefore the capture coefficient. The working mechanism underlying the possible increase in the measured cryopumping speed due to non-condensable gases is discussed in Chapter I.

Insufficient data was collected to form conclusions for liquid helium cryopumping utilizing nitrogen gas. The 75% uncertainty in the experimental run for a $\dot{V}_0$ of 1 cc/min was due largely to an uncertainty in the flow measurement (67%) and pressure measurement (70%). Therefore, future investigations employing the existing instrumentation must use higher gas flowrates, preferably large enough to produce equilibrium chamber pressures in the 10^{-5} Torr region.

A very substantial initial transient behavior was observed for the test runs with CO_2. During this transient period, the measured cryosurface pumping speed was very low. However, if a CO_2 flowrate of

approximately 1 cc/min was introduced into the chamber for thirty minutes prior to measuring the cryosurface pumping speed, this transient effect was not observed. This suggests that the cryosurface must be precoated with a layer of solid condensate before a steady state condition exists. Wang (26) also observed this behavior and referred to it as a "bare" surface effect.

10. Conclusions.

a) The experimental procedure employed appears adequate for collecting the necessary data to evaluate cryopumping speeds and capture coefficients.

b) The uncertainty interval for the experimental results can be reduced by introducing high enough gas flowrates (CO_2 and N_2) to obtain chamber equilibrium pressures in the 10^{-5} torr range.

c) More experimental runs are necessary with liquid helium cryopumping before a conclusive capture coefficient can be reported for nitrogen gas.

d) A chamber pressure of 5×10^{-8} torr was obtained with cryopumping.

This corresponds to approximately 520 Kilometers (323 miles), therefore, the chamber may be used to simulate outer space for a specimen exhibiting negligible outgassing.

BIBLIOGRAPHY

1. Bailey, B. M., and Chaun, R. L., 1958 Vacuum Symposium Transactions, 262, Pergamon Press, Inc., 1959.

2. Barrington, A. E., High Vacuum Engineering, New Jersey, Prentice Hall, Inc., 1963.

3. Blears, Greer, Nightingale. 1960 Vacuum Symposium Transactions, Pergamon Press, Inc., 1961.

4. Bell, J. H. Jr., Cryogenic Engineering, New Jersey, Prentice Hall, Inc., 1963.

5. Chaun, R. L., and Wallance, D., "Present Status of Cryopumping", USCEC Memorandum No. 1, November, 1960.

6. Chaun, R. L., "A Study of the Condensation of Nitrogen Below the Triple Point", USCEC Rept 56-201, AFOSR TN 57-19, AD 115-052, 28 February, 1957.

7. Crockett, A. H., and Din, F., Low Temperature Techniques, New York, Interscience Publishers, Inc., 1960.

8. Dayton, 1959 Vacuum Symposium Transactions, Pergamon Press, Inc., 1960.

9. Dushman, S., Scientific Foundations of Vacuum Technique, New York, John Wiley and Sons, Inc., 2nd edition, 1962.

10. Faires, V. M., Thermodynamics, 4th edition, New York, McMillian Co., 1962.

11. Guthrie, A., Vacuum Technology, New York, John Wiley and Sons, Inc., 1963.

12. Guthrie, A., and Wakerling, R. K., Vacuum Equipment and Techniques, New York, McGraw Hill Book Co., Inc., 1949.

13. Hoenig, M. O., "Development of Modular Cryopump", Advance in Cryogenic Engineering, Vol. 9, Plenum Press, 1964.

14. Kreith, F., Principles of Heat Transfer, Pennsylvania, International Textbook Co., 1959.

15. Karamcheti, K., "A Study of the Condensation of Nitrogen Below the Triple Point", USCEC Rept 56-201, AFOSR TN 57-19, AD 115-052, 28 February, 1957.

16. LaChance, G, M., "The Theory and Construction of a Liquid Helium Cryogenic Pump", thesis, U. S. Naval Postgraduate School, 1964.

17. Lapelle, R. R., and Lerner, M., Ultra High Vacuum Theory and Design, The Boeing Company, 1963.

18. Markley, Roman, Vosecek. 1961 Vacuum Symposium Transactions, Pergamon Press, Inc., 1962.

19. Moore, R. W., "Cryopumping in the Free Molecular Flow Regime", Mass., Arthur D. Little, Inc., 1962.

20. Naundorf, C. H., 1960 Vacuum Symposium Transactions, 60, New York, Pergamon Press, Inc., 1961.

21. Scott, R. B., Cryogenic Engineering, New Jersey, D. Van Nostrand Company, Inc., 1959.

22. Steinherz, H. A., Handbook of High Vacuum Engineering, New York, Reinhold Publishing Corporation, 1963.

23. Training Section of the Boeing Company, Practical Vacuum System Design, 1962.

24. Vance, R. W., and Duke, W. M., Applied Cryogenic Engineering, New York, John Wiley and Sons, Inc., 1962.

25. Wang, E. S. J., Collins, J. A. Jr., and Haygood, J. D., Advances in Cryogenic Engineering, Vol. 8, 73, Plenum Press, 1963.

26. Wang, E. S. J., Collins, J. A. Jr., and Haygood, J. D., Advances in Cryogenic Engineering, Vol. 7, 44, Plenum Press, 1962.

27. Yarwood, J., and Pirani, M., Principles of High Vacuum Engineering, London, Chapman and Hall, LTD., 1961.

28. Powell, R. L., Bunch, M. D., and Caywood, L. P., Advances in Cryogenic Engineering, Vol. 6, 537, Plenum Press, 1961.

29. Dawson, J. P., Haygood, J. D., and Collins, J. A. Jr., Advances in Cryogenic Engineering, Vol. 9, 443, Plenum Press, 1964.

30. Dawson, J. P., "Prediction of Cryopumping Speeds in Space Simulation Chambers", (to be published).

31. Kline, S. J., and McClintock, F. A., "Uncertainties in Single-Sample Experiments", Mechanical Engineering, January, 1953, pp. 3-8.

Figure 3

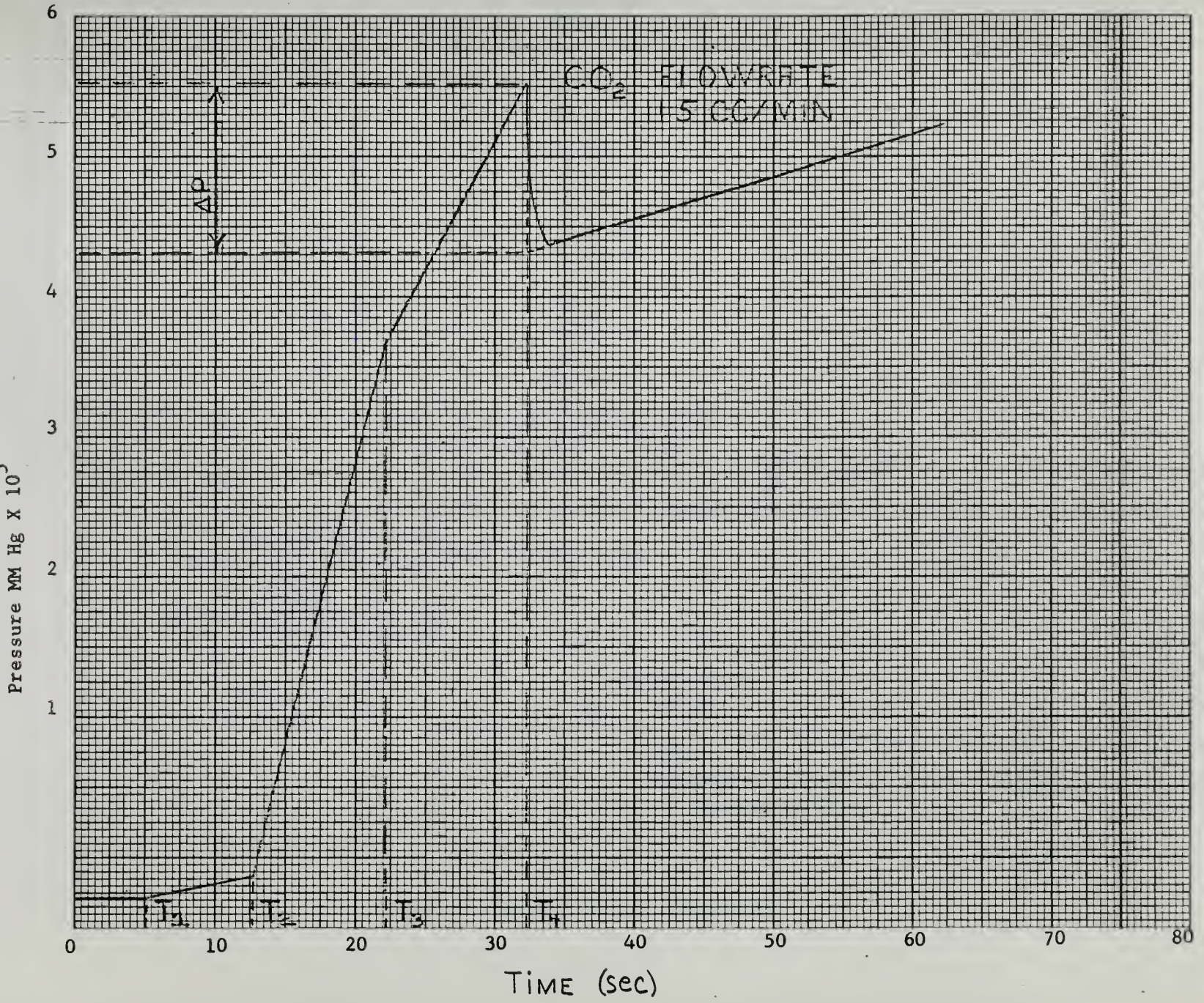
CO_2 FLOWRATE
15 CC/MIN
ΔP
T_1
T_2
T_3
T_4
Pressure MM Hg X 10^5
Time (sec)
0
10
20
30
40
50
60
70
80
1
2
3
4
5
6

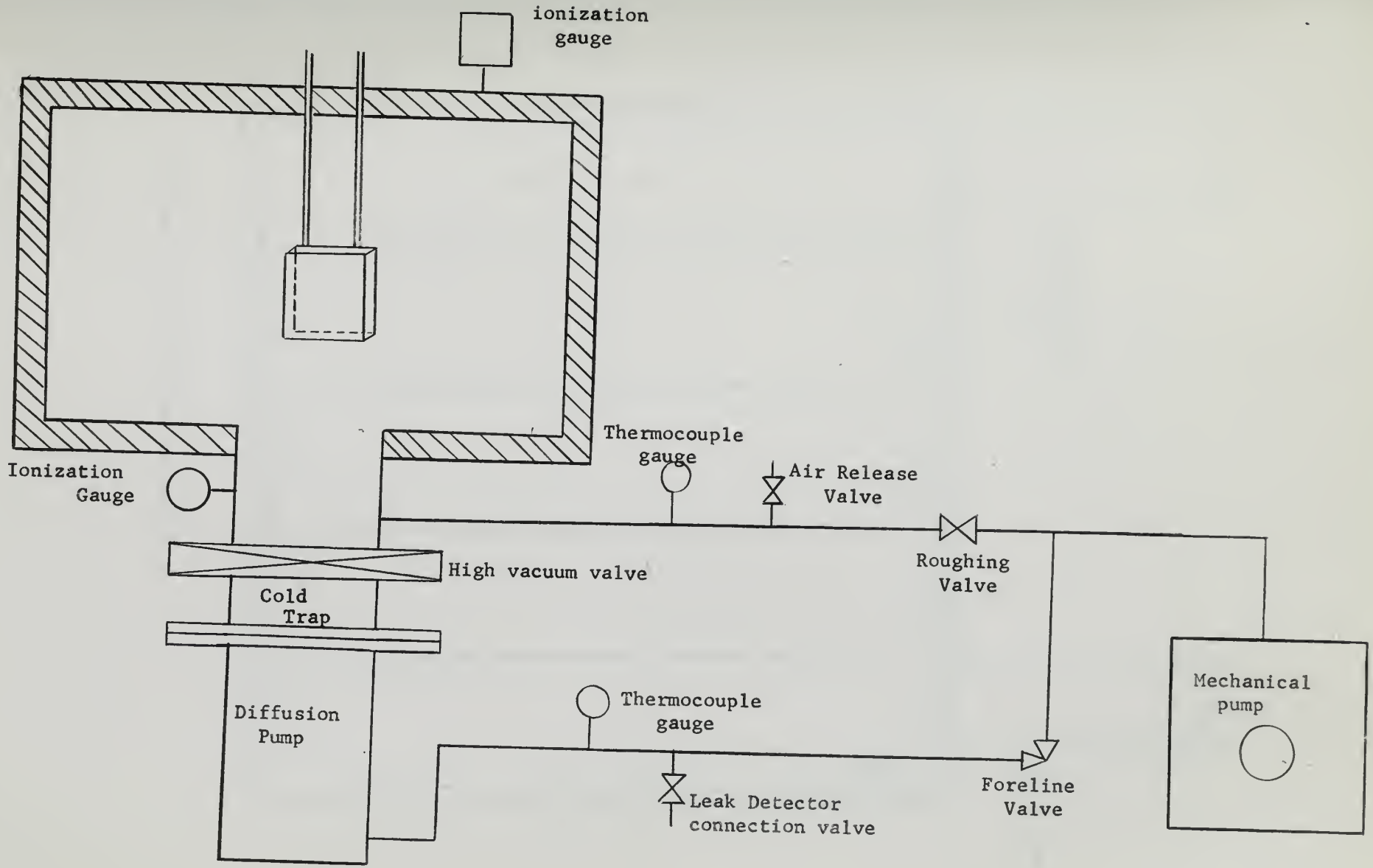

Figure 4 Pumping System Schemmatic

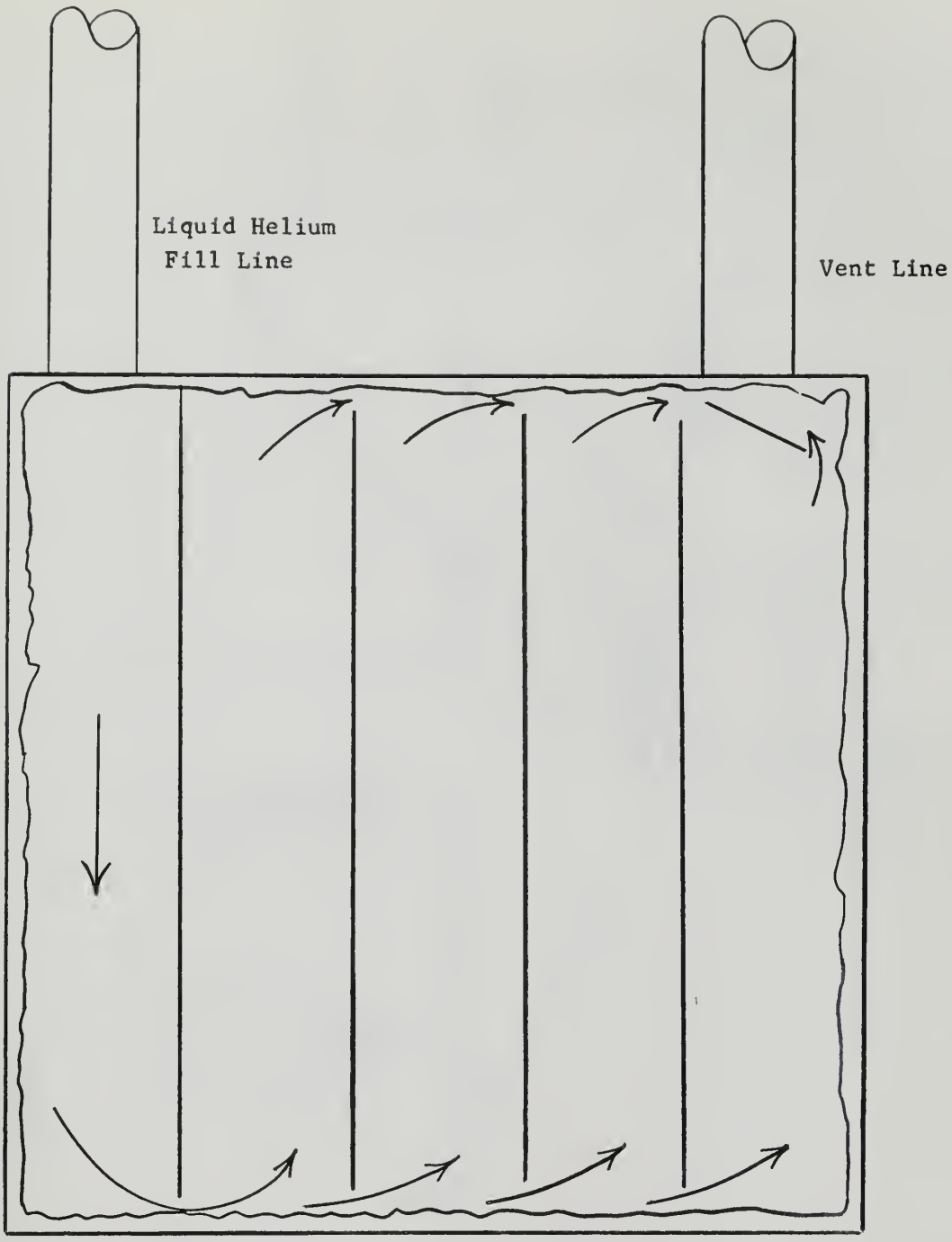

Figure 5 Liquid Helium Cryopanel

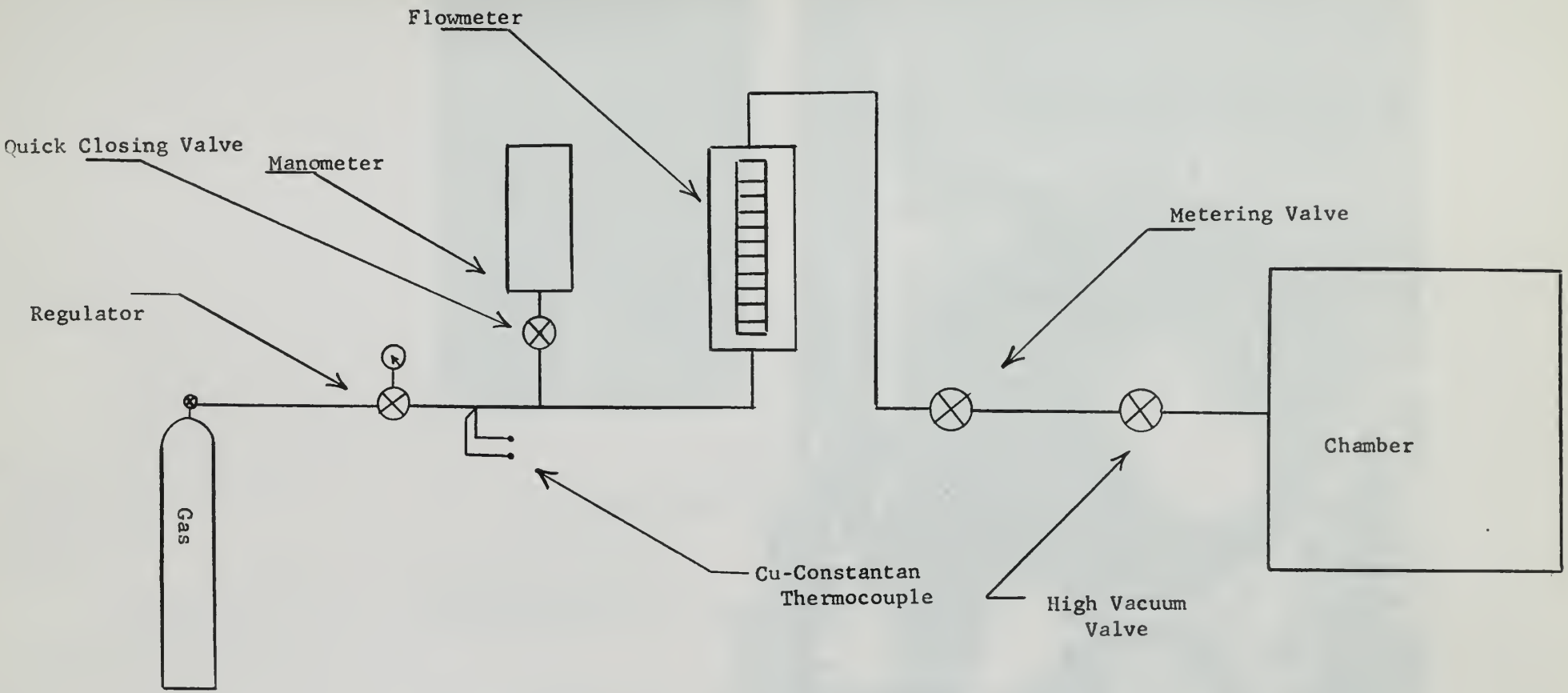

Figure 6 Gas Metering System

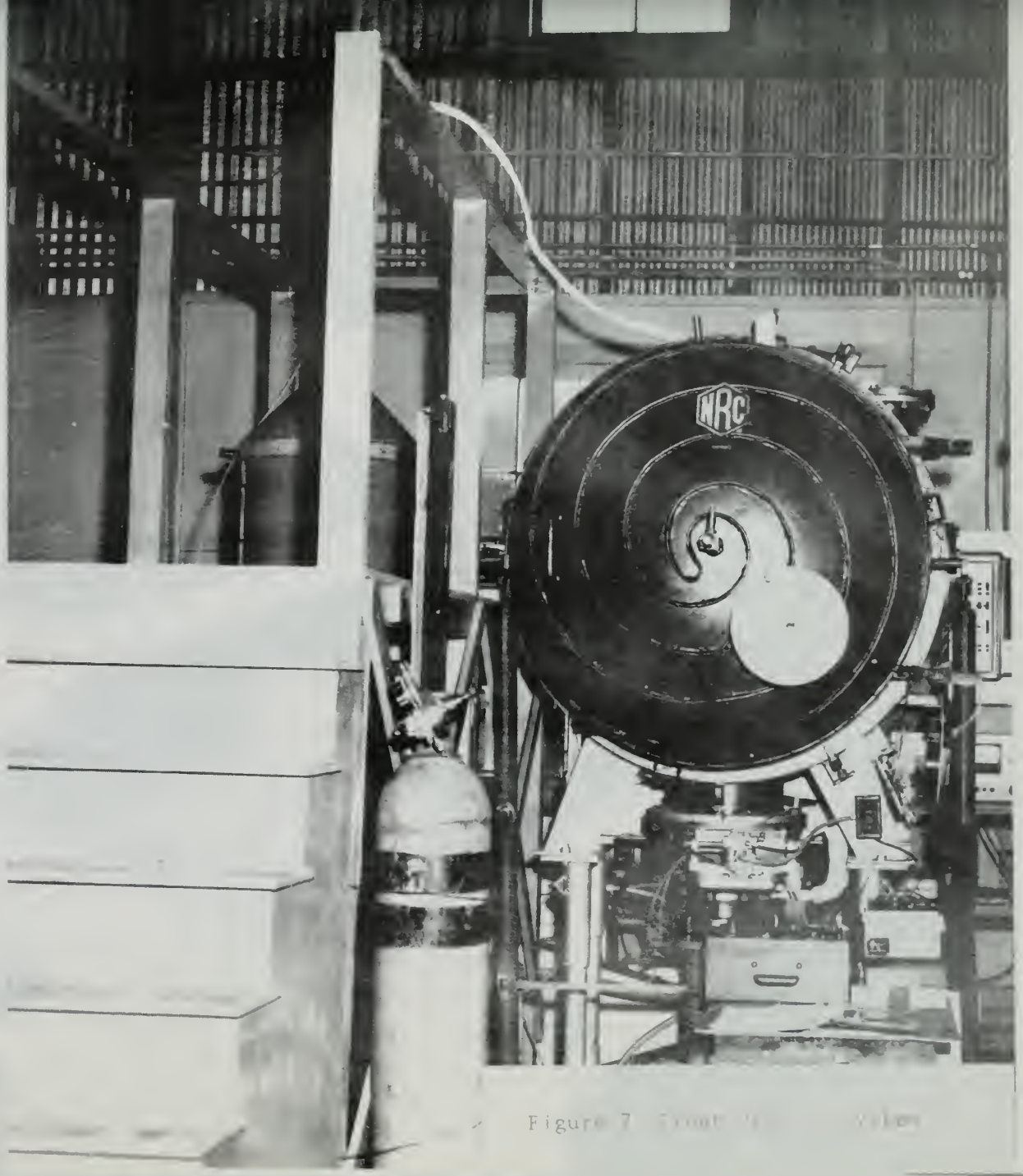

Figure 7 [illegible] Valve

Figure [illegible] Mounting Plate

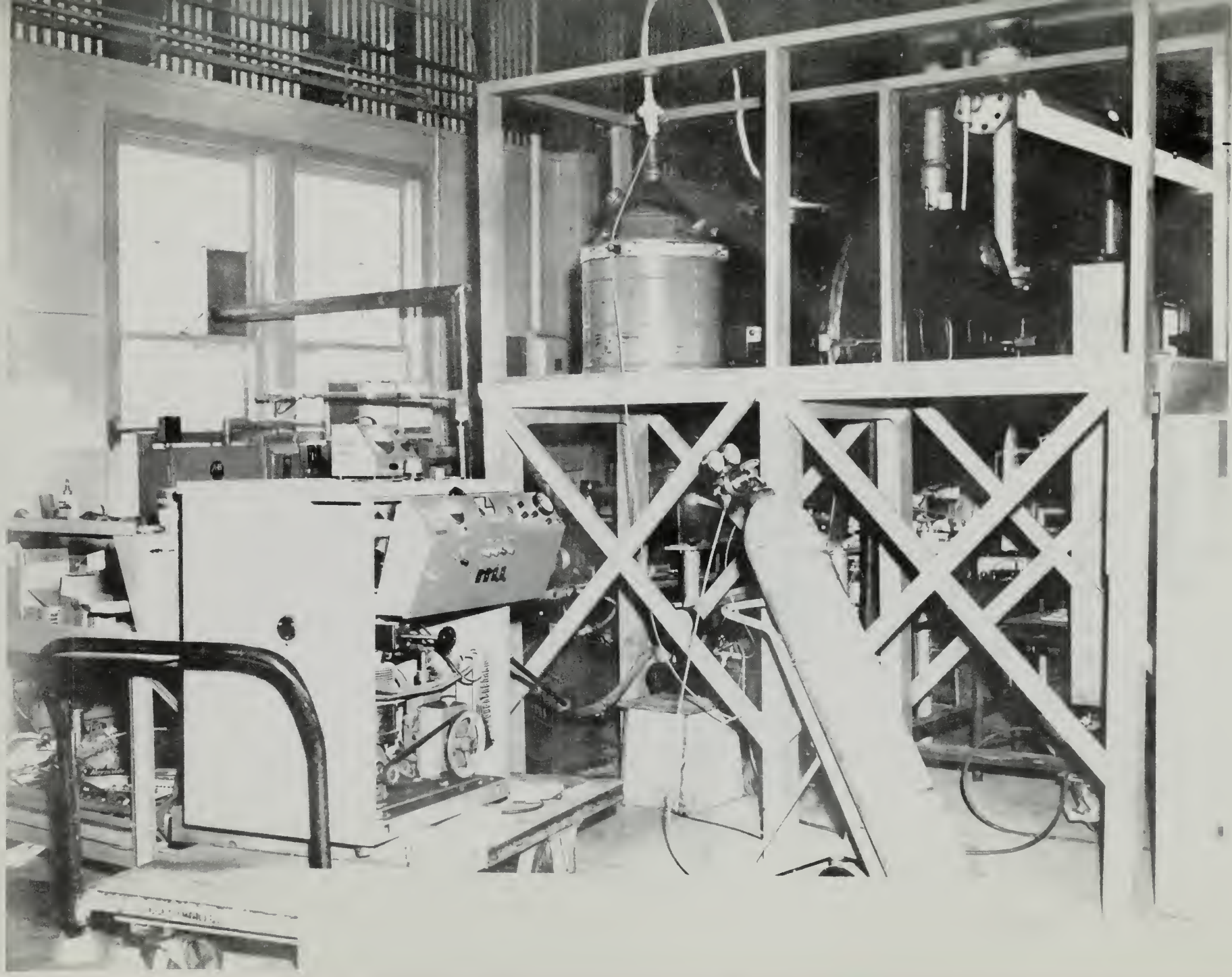

APPENDIX I (a)

System Dimensions

A. Length:

Chamber diameter	41 in. = 104 cm.
Chamber length	46 in. = 116.6 cm.
Cylindrical Shield Diameter	33 in. = 83.7 cm.
Cylindrical Shield Length	36 in. = 91.3 cm.
Shield End Panel Diameter	36 in. = 91.3 cm.

B. Area:

Chamber Walls	$8.56 \times 10^3 in^2 = 5.51 \times 10^4 cm^2$
Heat Shield*	$5.44 \times 10^3 in^2 = 3.51 \times 10^4 cm^2$
Stainless Steel (304) Cryopanel	$2.88 \times 10^2 in^2 = 1.856 \times 10^3 cm^2$

*Projected surface area, does not include embossing.

C. Volume:

Chamber	$6.06 \times 10^4 in^3$ = 994 Liters

APPENDIX I (b)

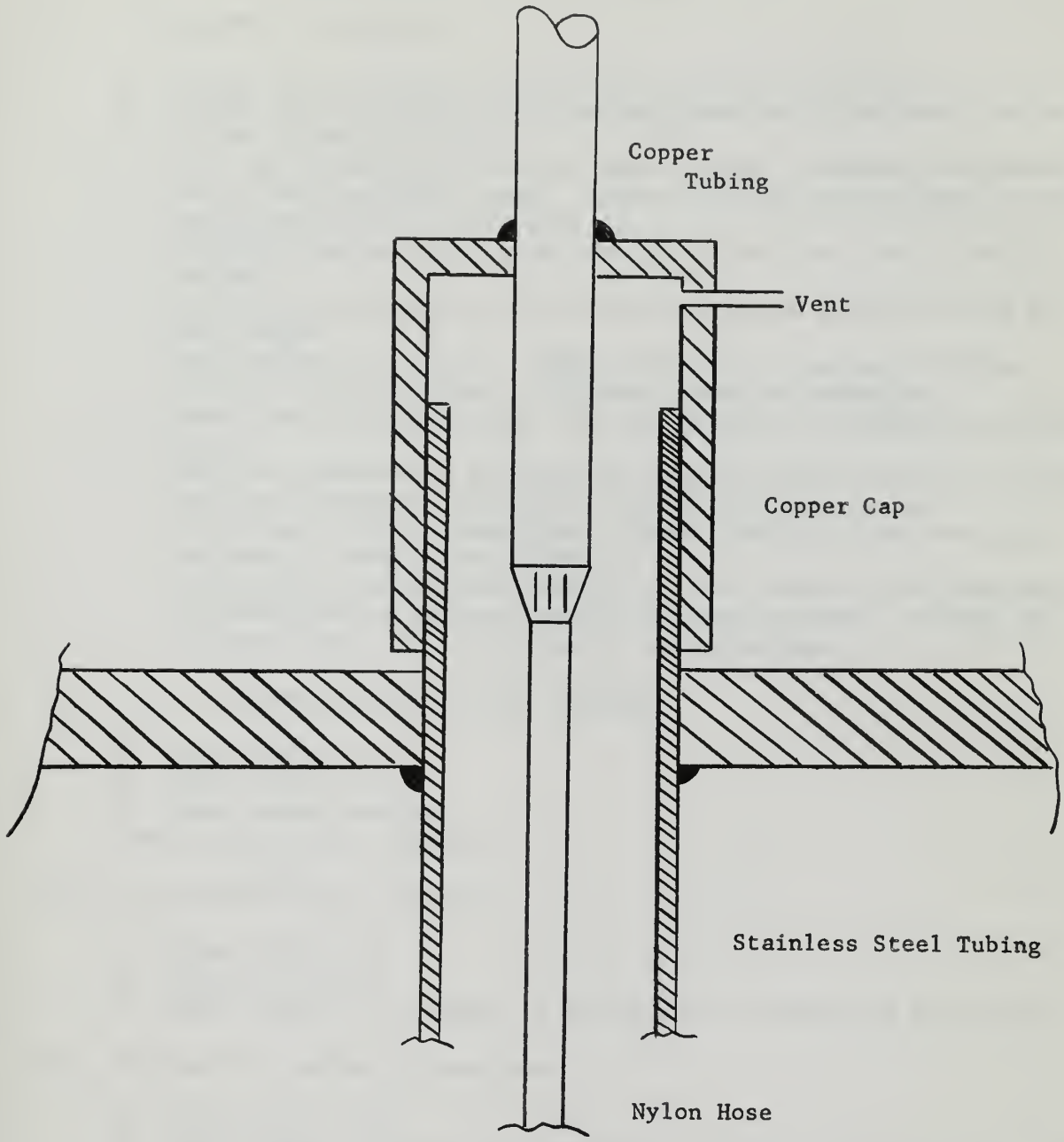

Liquid Nitrogen Feedthrough

APPENDIX II

Pumping System Operating Procedure

I. To evacuate the chamber:

A. Insure air is available to actuate valves V-2 and V-1.
B. Place the individual electrical switches for the solenoid valves in the closed position.
C. Turn on the cooling water for the cold cap, diffusion pump cooling coils, and mechanical pump. Insure that the cooling water to the quick quench coils is secured.
D. Energize the controllers for the mechanical pump, and solenoid valves.
E. Insure that all doors, ports, and air release valves V-4 and V-5 are closed.
F. Open valves V-3 and V-2. NOTE: Valve V-2 is operated with an electric switch. There is no manual mode of operation.
G. Start the mechanical pump, thus evacuating the chamber and diffusion pump.
H. When the pressure in the foreline reaches approximately 70 microns or lower, energize the heaters for the diffusion pump.
I. After twenty (20) minutes have elapsed, the diffusion pump will be ready to pump on the chamber.
J. Close valve V-3 and open valve V-1. The system is now completely in operation and the gas flow is now from the tank, through the diffusion pump, to the mechanical roughing pump.

II. If it is necessary to open the chamber:

A. Close Valve V-1.
B. Open valve V-5.
C. Leave pumps running.

The tank may now be opened.

III. To re-evacuate the chamber:

A. Close Valve V-5.
B. Open Valve V-3.
C. When pressure in chamber is 70 microns or lower open Valve V-1.

IV. To shut the pumping system down:

A. Close Valve V-1.
B. De-energize diffusion pump heaters and turn on the quick cool water.
C. Wait approximately 15 minutes for the diffusion pump to cool.
D. Open Valve V-5.
E. After diffusion pump has cooled down (approximately 15 minutes), close Valve V-2.
F. Secure roughing pump and open valve V-3 immediately.
G. Secure all cooling water supplies.
H. De-energize all controllers.
I. System is now secured.

APPENDIX III (a)

Shielding Calculations

a) Cryopanel

The radiation heat load on the unshielded cryopanel may be calculated by assuming the panel to be a gray body within a gray body enclosure. A reasonable value for the emissivity of the chamber walls at 300 ^{o}K is .40 and for the cryopanel at 20 ^{o}K, a value of .20 (5). The electric analog is a simple series circuit (14).

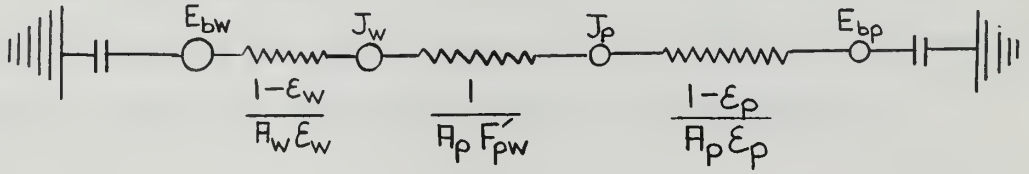

and the heat load may be found as follows

$$q/A_p = F_{pw}(E_{bw} - E_{bp}) \tag{1}$$

where:

$$F_{pw}A_p = \frac{1}{\frac{1-\varepsilon_w}{A_p\varepsilon_w} + \frac{1}{F'_{pw}A_p} + \frac{1-\varepsilon_p}{A_w\varepsilon_p}} \tag{1a}$$

$$E_b = \sigma T^4 \tag{1b}$$

Solving (1) for q/A_p gives .0320 watts/cm^2 for the radiation heat load on the unshielded cryopanel.

In order to reduce the radiation heat load on the panel, a stainless steel heat shield filled with liquid air, 33" in diameter, 36" long, and with an emissivity of approximately .4 is placed between the wall and panel.

By a similar calculation to the one above, the heat load on the panel is found to be 1.35×10^{-4} watts/cm^2. This is .42% of the unshielded radiation heat load on the panel and greatly reduces the helium loss due to radiant heat.

b) Liquid Nitrogen Heat Shield.

Since a batch process is to be used for filling the liquid nitrogen heat shield, a means for reducing the radiation heat load on this shield would be both practical and economical.

The radiation heat load on the liquid nitrogen shield may be calculated by assuming the chamber wall and the shield to be flat parallel plates. Neglecting end effects, equation (1a) reduces to:

$$F_{SW} = \frac{1}{\frac{1}{\varepsilon_S} + \frac{1}{\varepsilon_W} + 1} \qquad (2)$$

Utilizing equation (1), and assuming the emissivity of the chamber walls as .40 at 300 ^{o}K and the emissivity of the stainless steel heat shield as .20 at 77 ^{o}K, the heat load q/A, is calculated to be 4.19×10^{-3} watts/cm^2.

If a dry aluminum heat shield is placed between the walls and the liquid nitrogen shield, one would expect the radiant heat load on the nitrogen shield to be substantially reduced. The end result would be a smaller liquid nitrogen consumption and a longer operating time per charge.

In order to calculate the reduction of radiant heat on the nitrogen shield, a value of .10 for both sides of the aluminum shield will be assumed. The electric analog is a simple series circuit (14):

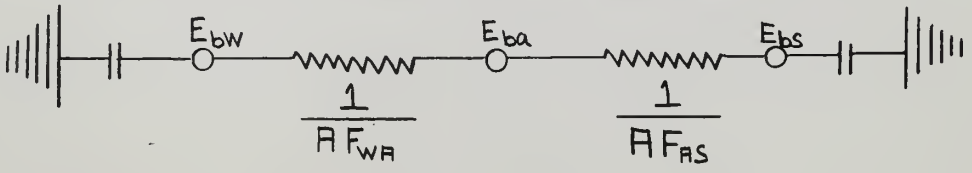

and the heat load may be found:

$$q/A = \frac{E_{bW} - E_{bS}}{\frac{1}{F_{WA}} + \frac{1}{F_{AS}}} \tag{3}$$

where:

$$F_{WA} = \frac{1}{\frac{1}{\varepsilon_W} + \frac{1}{\varepsilon_A} - 1} \tag{3a}$$

and:

$$F_{AS} = \frac{1}{\frac{1}{\varepsilon_A} + \frac{1}{\varepsilon_S} - 1} \tag{3b}$$

Utilizing equations (3) through (3b), the radiation heat load on the liquid nitrogen shield with the dry aluminum heat shield installed is found to be 1.06×10^{-3} watts/cm^2. The net effect is a 25% reduction of the heat load on the liquid nitrogen filled shield.

APPENDIX III (b)

Cryopanel Calculations

As the solid condensed gas forms on the cryopanel area, the thermal conductivity of the solid coating and its increasing thickness will affect further condensation of the gas. In designing the cryopanel, the freezing area provided should be adequate so that during the entire test run period the rate of solid formation will be maintained at a value greater than or equal to the total mass flow rate into the chamber.

The rate of solid formation on the cryopanel surface can be treated as a one - dimensional heat conduction process with a time dependent boundary condition at the vapor - solid interface. Both Chaun (6) and Karamcheti (15) have solved this problem utilizing data from A. D. Little Co. to determine the thermal conductivity of solid nitrogen.

The rate of solid formation on the cryopanel surface is (15).

$$\dot{M} = b\rho\sqrt{\frac{k}{\rho C}}\,\frac{1}{\sqrt{t}} \qquad (1)$$

where $b = 0.2325$ (a constant)

$\rho = 1.0$ grams/cc for solid nitrogen

$k = 2.455 \times 10^{-4}$ cal/sec cm °K

$C = .39$ cal/gm °K

The constant, b, was determined from the following equation

$$be^{b^2}\,\mathrm{erf}\,b = \frac{1}{\sqrt{\pi}}\,\frac{C}{L}\,(T_S - T_R) \qquad (2)$$

where T_s = temperature at vapor - solid interface 28 ^{o}K

T_r = temperature of cold surface 20 ^{o}K

L = latent heat of condensation from the gas phase to the solid phase, 60 CAL/gram.

The temperature at the vapor - solid interface is the saturation temperature of solid nitrogen corresponding to 10^{-6} mm Hg.

Assuming a volume flowrate of 1000 cc/min and negligible outgassing, the mass flowrate of nitrogen gas into the chamber can be computed. The density can be computed as follows:

$$\rho = \frac{W}{V} = \frac{PM}{R_o T} \tag{3}$$

$$\rho = 1.6035 \times 10^{-5} \frac{MP(\text{torr})}{T} \quad \text{gram cc}^{-1} \tag{3a}$$

where $R_0 = 62.364 \quad \frac{\text{mm Liter}}{^{o}K \ \text{gr - mole}}$

Equation (3) yields a value of 1.035 X 10^{-4} grams cc^{-1} for the density. Since the area of the cryopanel is 1854 cm^2, the mass flowrate is 3.35 X 10^{-4} grams sec^{-1} cm^{-2}. Substituting this value for G into equation (1) and solving for t we obtain

$$t = \left(\frac{b\rho}{G}\right)^2 \frac{k}{\rho c} \tag{4}$$

or t = 8.3 hours

Therefore in order to maintain the rate of solid formation greater than or equal to the total mass flow rate into the chamber, the maximum continuous run time is 8.3 hours. A more conservative maximum run time is 4 hours to allow for outgassing condensation, variations in thermal conductivity, etc.

Assuming a run time of 4 hours, the condensate thickness may be calculated (15).

$$X = 2b\sqrt{\frac{k}{\rho c}}\sqrt{t} \quad \text{CM} \tag{5}$$

where x = thickness of the condensate layer

Solving equation (5) for x yields a value of 1.4 cm.

It is now of interest to compute the liquid helium requirement due to the gas condensation load.

$$q_g = G\left[L + c_p(T_e - T_c)\right] \tag{6}$$

where G = mass flow rate into chamber grams/cc

L = latent heat 60 CAL/gram

C_p = entrance temperature of gas

T_e = entrance temperature of gas

T_c = temperature at vapor - solid interface

then $q_g = (3.35 \times 10^{-4}) \left[(60 + \frac{6.93}{28} (300-28)\right]$

$= .0427$ CAL/sec

and

$$V_{lhe} = \frac{q_g \, t}{L_H \quad H} \tag{7}$$

where

L_H = latent heat of vaporization of liquid helium

$_H$ = density liquid helium

$$V_{lhe} = \frac{(.0427)\ (4)\ (3600)}{(4.93)\ (125.1)}$$

= 1.085 Liters Liquid Helium

The radiation load on the cyropanel (App III(a)) is 1.67×10^{-4} watts/cm^2. Using this value for q in equation (7) yields a liquid helium requirement of 68.6 liters. Therefore, from the standpoint of liquid helium consumption we see that a 4 hour run time is not feasible. Therefore, a run time of 10 minutes corresponding to a liquid helium consumption of 2.86 liters for radiation was decided upon. A run time of 10 minutes is also sufficient time to allow equilibrium conditions to be established within the chamber.

APPENDIX III (c)

Pumpdown Time Calculations

A. Roughing Pumpdown Time.

The roughing time is defined as the time to pumpdown the chamber from 760 to .001 torr. This is accomplished by a 100 cfm mechanical pump connected via 3½ feet of stainless steel tubing to the chamber. It is necessary to rough the chamber down to at least 70 microns before the diffusion pump can be placed in operation. The pressure of 70 microns is the maximum allowable foreline pressure for the diffusion pump.

The throughput from the chamber is

$$Q = V \frac{dP}{dt} \tag{1}$$

where Q is expressed in Torr Liters sec^{-1}, V, the volume of the chamber in liters, and $\frac{dp}{dt}$, the rate of change of pressure with time, in torr sec^{-1}.

The throughput entering the pump is

$$Q = SP \tag{2}$$

where S is the pump speed (Liters/sec) and P is the pressure in torr.

Equating equations (1) and (2) and integrating we obtain

$$\Delta t_R = \frac{V}{S} \text{LN } P_1/P_2 \tag{3}$$

where Δt_R is the roughing time or time to pumpdown from pressure P_1 to pressure P_2.

Equation (3) may be modified by a factor, K, to account for outgassing in the pressure range below 1 torr. This factor is deduced from the analysis of a large amount of empirical data. The values for a clean mild-steel tank are tabulated below (22).

$$\Delta t_R = \frac{KV}{S} \text{ LN } \frac{P_1}{P_2} \qquad (3a)$$

where

Pressure Range	K
760 to 1.0 torr	1.1
1 to 0.1 torr	1.5
0.1 to .001 torr	4.0

Substituting into equation (3a) for each pressure range and summing the three results yields a theoretical roughing time of 12½ minutes. This theoretical time compares favorably with the actual time of 15 minutes.

B. Pumpdown Calculation - Below 10^{-4} torr.

Pumpdown time calculations in the high vacuum range are extremely difficult because the absorption gas load is so sensitive to uncontrollable chamber surface conditions (22).

The pumping speed at the chamber can be obtained from

$$\frac{1}{S_P} = \frac{1}{S_D} + \frac{1}{U_B} + \frac{1}{U_V} \qquad (4)$$

therefore

$$S_P = \frac{S_D U_B U_V}{S_D + U_B + U_V} \quad \text{Liter sec}^{-1} \qquad (4a)$$

where

S_p = Pumping speed at chamber

S_d = Diffusion Pump Speed

U = Conductance of cold trap

U_V = Conductance of valve

Solving equation (4a) yields a pumping speed at the chamber of 600 Liters/sec.

The pumpdown time from 10^{-4} torr to lower pressures can be calculated from a generalized version of one proposed by Naundorf (20). See Figure (10). This procedure is based on the following assumptions:

1. Pumping speed constant versus pressure.
2. Outgassing of chamber versus time of the form Q = k/t - linear with a -45 slope on a log - log plot.
3. Negligible leaks
4. Negligible gasket outgassing

Utilizing this method the time required to pumpdown from 10^{-4} to 5 X 10^{-6} torr can be calculated. From Figure (10) the time value of .07 hours is obtained for a mild steel chamber. The pumpdown time, t_d, is

$$t_D = 0.07 \times A_p/S_p \qquad (5)$$

where

A_p= surface area of chamber - cm^2

S_p = pumping speed at chamber - Liters/sec

then

$$t_d = \frac{.07 \times 5.51 \times 10^4}{600}$$

t_d = 6.42 hrs.

The actual time required is 8 hours. However, the theoretical calculation neglected gasket outgassing. Also note that the value of 8 hours is for a warm chamber. Utilizing liquid nitrogen the chamber can be pumped down in approximately 2 hours from atmospheric pressure to less than 1 X 10^{-6} Torr.

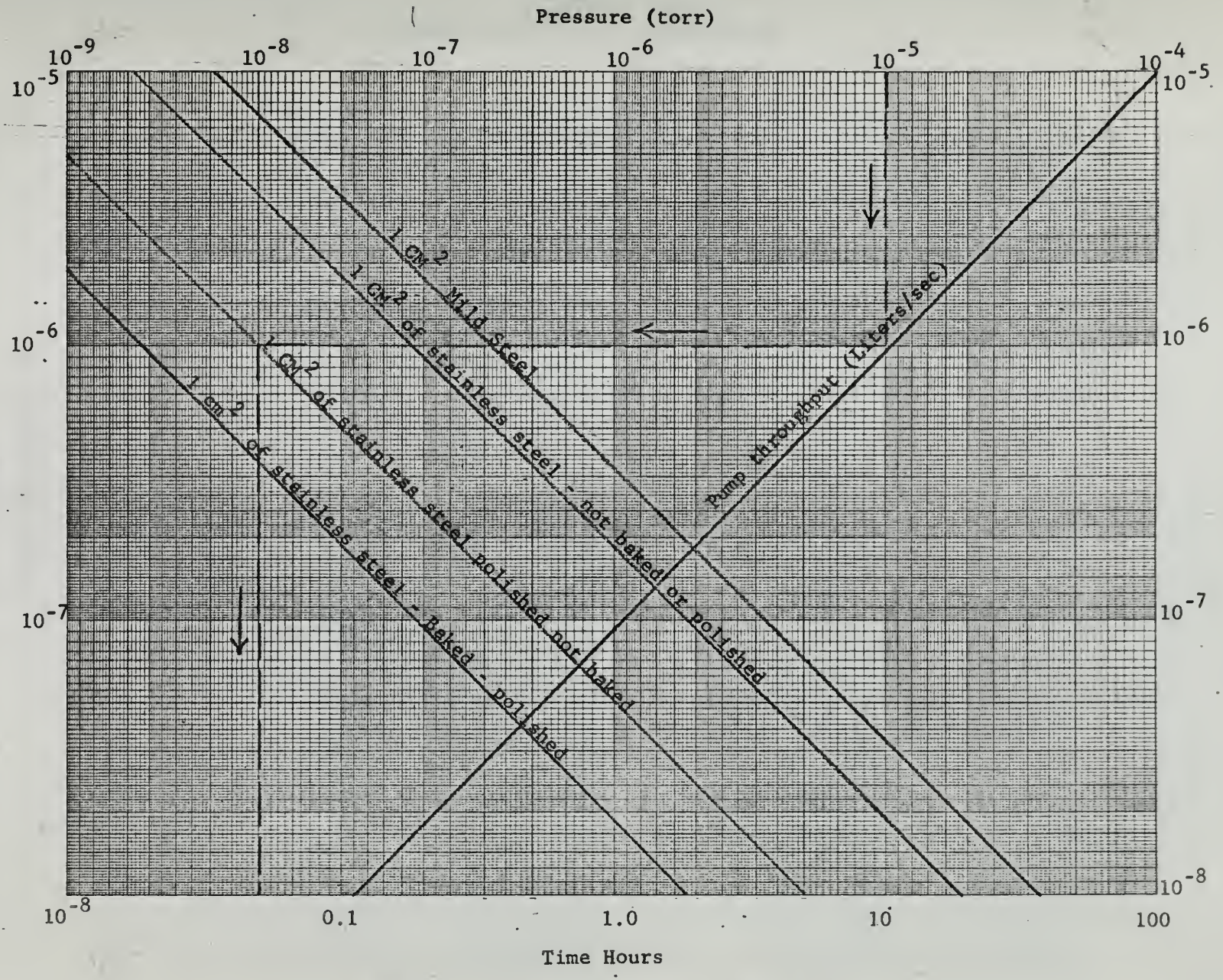

Figure 10 Outgassing rate versus Time

APPENDIX IV (a)

Vapor Pressure vs. Temperature

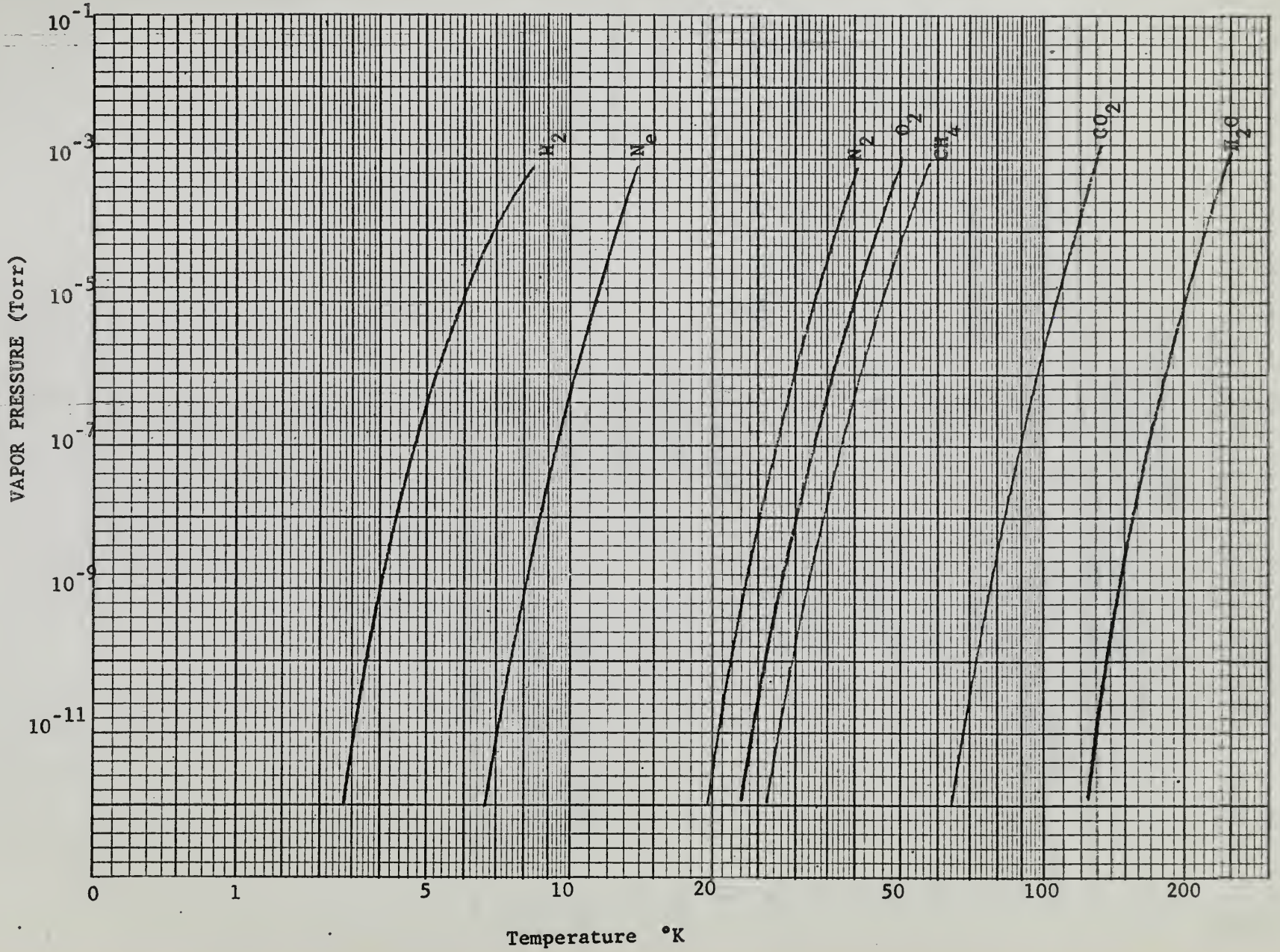

APPENDIX IV (b)

Outgassing Data

Material	Condition	Outgassing Rate $\frac{\text{Torr - L}}{\text{sec} \quad \text{cm}^2}$ 1 hr.	10 hr.	100 hr.	Source
Mild Steel	shot blasted		6×10^{-8}		(3)
Neoprene		3×10^{-5}	1.5×10^{-5}		(3)
Stainless Steel		2×10^{-7}	2×10^{-8}		(3)
Aluminum	anodized		1×10^{-7}		(8)
Brass	cast washed		3×10^{-7}		(8)
Copper		2.3×10^{-6}			(8)
Silver		6×10^{-7}			(8)
Butyl Rubber		1.5×10^{-6}			(8)
"Epon 828"	degassed	6.7×10^{-7}	5.9×10^{-8}	9.4×10^{-9}	(18)
Teflon		4.6×10^{-7}	2.1×10^{-7}	9×10^{-8}	(18)

APPENDIX IV (c)

0 - Ring Physical Properties

	Buna N	Silicone	Neoprene	Viton - A
Tensile Strength	2200 psi	600 psi	1800 psi	2100 psi
Elongation	300%	150%	300%	175%
Temp. Range	-65 to 250 F	-110 to 500 F	-65 to 250 F	4 to 400 F
Resistance to Tear	Fair	Fair	Good	Fair
Permeability to Gases	Medium	Medium	Low	Low
Resistance to water swelling	Excellent	Very good	Good	- - - -